Single cell transcriptomic analysis of the adult mouse pituitary reveals a novel multi-hormone cell cluster and physiologic demand-induced lineage plasticity

Yugong Ho[1,5,*]. Peng Hu[1,3,5], Michael T. Peel[1], Pablo G. Camara[1,4], Hao Wu[1,3,*], and Stephen A. Liebhaber[1,2,]

Departments of Genetics[1] and Medicine[2], Penn Epigenetics Institute[3], and Penn Institute for Biomedical Informatics[4], Perelman School of Medicine, University of Pennsylvania, Philadelphia, PA 19104

[5] These authors contributed equally

[*] Corresponding authors

Running title: Single cell transcriptomic analysis of the adult mouse pituitary

Abstract

The anterior pituitary gland drives a set of highly conserved physiologic processes in mammalian species. These hormonally-controlled processes are central to somatic growth, pubertal transformation, fertility, lactation, and metabolism. Current models, based on targeted immuno-histochemical and mRNA analyses, suggest that each of the seven hormones synthesized by the pituitary is produced by a specific and exclusive cell lineage. However, emerging evidence suggests a more complex model in which critical aspects of hormone specificity and plasticity of pituitary cells remain undefined. Here we have applied massively parallel single-cell RNA sequencing (scRNA-seq), in conjunction with a set of orthogonal imaging studies, to systematically map the cellular composition of adult male and female mouse pituitaries at single-cell resolution and in the setting of major physiologic demands. These analyses reveal sex-specific cellular diversity associated with normal pituitary homeostasis, and identify an array of specific hormone-enriched cell-types and a series of non-hormone producing interstitial and supporting cell lineages. Unexpectedly, scRNA-seq further uncovers the presence of a major cell cluster that is characterized by a unique multi-hormone gene expression profile. The detection of dynamic shifts in cellular representations and transcriptome profiles within a number of these clusters in response to well-defined physiologic demands suggests their corresponding roles in cellular plasticity. These studies point to an unanticipated complexity and plasticity in pituitary cellular composition that may serve to expand upon current models and concepts of pituitary hormone gene expression.

Introduction

The pituitary is a key regulatory gland in mammalian organisms. Complex arrays of hormonal outputs from the pituitary play central roles in physiological pathways and a wide array of inherited and acquired pathologic processes (Kelberman et al., 2009). These pathways impact post-natal growth, puberty, fertility, lactation, and metabolism. The pituitary contains a posterior lobe that comprises a direct extension of the central nervous system, and an anterior/median lobe (referred herein as anterior lobe) that is derived from epithelial cells of the oropharynx (Davis et al., 2013). The anterior pituitary contains cells that synthesize growth hormone (GH), prolactin (PRL), thyroid-stimulating hormone β subunit (TSHβ), adrenocorticotrophic hormone (ACTH), luteinizing hormone β-subunit, (LHβ), follicle-stimulating hormone β-subunit (FSHβ), and α melanocyte-stimulating hormone (α-MSH) (**Fig. S1**) (Zhu et al., 2007). Hormone synthesis and release from the anterior pituitary is coordinated by regulatory factors generated within signaling centers in the hypothalamus and transmitted to the pituitary *via* a dedicated hypothalamic-pituitary portal circulatory system (Vazquez-Borrego et al., 2018). A complete understanding of how these regulatory networks impact physiologic function requires defining the composition and relationships of cell lineages of the anterior pituitary and their corresponding patterns of hormone gene expression in an unbiased and comprehensive manner.

The prevailing model of anterior pituitary structure and function is predominantly based on the assumption that each hormone is expressed from a distinct cell type (Davis et al., 2013; Zhu et al., 2007). This model predicts that the seven major hormones secreted by the anterior pituitary are synthesized by a set of six corresponding cell

lineages (in this model the two gonadotrope hormones, FSHβ and LHβ, are co-expressed from a single lineage) (**Fig. S1**). While compelling in many respects, this model remains to be fully tested as it is based on targeted immuno-histochemical and mRNA-based analyses. The varying sensitivities and specificities of these approaches (Nakane, 1970), their inductive nature, and their limited capacity to examine multiple hormonal expressions within single cells, suggest that they may not be fully informative. The possibility of a more complex composition of pituitary cell lineages and hormone expression is further suggested by a number of reports of pituitary cells that express multiple hormones (Seuntjens et al., 2002a; Villalobos et al., 2004a, b). In addition, reports of pituitary cells with mitotic markers and factors linked to stem cell functions have been used to support complex models of pituitary dynamics linked to cellular expansion, *trans*-differentiation, and lineage plasticity (Frawley and Boockfor, 1991; Vidal et al., 2001; Villalobos et al., 2004b). Such complex relationships of pituitary cell types are supported by a limited number of lineage tracing studies (Castrique et al., 2010; Fu and Vankelecom, 2012; Luque et al., 2007). Thus, the degree to which the current model of hormone expression fully encompasses pituitary structure and function remains open to further study and could be facilitated by assignment and cataloging of the gene expression profiles of individual cells in the pituitary using a comprehensive and unbiased approach.

The advent of single cell technologies has facilitated the analysis of cell lineages within a rapidly expanding array of tissues and has been used to effectively explore how defined cell lineages in various tissues respond to physiologic stresses and mediate specific functions (Tanay and Regev, 2017). Newly developed approaches of single cell

isolation linked to high-throughput RNA sequencing approaches, such as Drop-Seq and 10X Genomics platforms (Macosko et al., 2015; Zheng et al., 2017), can now be applied to massively parallel analysis of single cell transcriptomes. These comprehensive and unbiased approaches can be of particular value in uncovering cellular heterogeneity and novel cell types, and in revealing corresponding regulatory factors involved in lineage differentiation and function (Campbell et al., 2017; Chen et al., 2017; Hu et al., 2017; Shekhar et al., 2016).

In the current study, we have applied Drop-seq technology (Macosko et al., 2015), in conjunction with a set of orthogonal single cell protein and RNA-based validation approaches, to define the steady state cellular composition of the adult mouse anterior pituitary at single cell resolution. Our data are concordant with certain aspects of current models, most notably in the identification of individual cell clusters expressing specific pituitary hormones and by highlighting patterns of sexual dimorphism in the pituitary cell compositions. Remarkably, these data also reveal the presence of a major cluster of multi-hormone expressing cells that contribute to the response of the pituitary to robust physiologic stresses linked to post-partum lactation and to stimulation by a hypothalamic regulatory factor. These analyses provide a comprehensive view of pituitary gene expression in adult pituitary and generate testable models of cell plasticity that underlie the capacity of the pituitary to respond to major physiologic demands.

Results

Unbiased scRNA-seq analysis reveals an unexpected complexity of hormone gene expression within *Pou1f1*$^{+}$ clusters.

Studies of the pituitary development and lineage differentiation have suggested a model in which each of six distinct hormone expressing cell lineages expresses a corresponding polypeptide hormone (**Fig. S1**) (Zhu et al., 2007). The differentiation of these cell lineages are controlled by a variety of transcription factors and signaling molecules (Kelberman et al., 2009). Multiple lines of genetic and biochemical evidence have converged on the conclusion that pituitary specific POU homeodomain transcription factor, Pou1f1, serves an essential function in driving terminal differentiation of cells expressing *Gh* (somatotropes), *Prl* (lactotropes), and *Tshb* (thyrotrope) ('Pou1f1 dependent lineages'; **Fig. S1**) (Camper et al., 1990; Li et al., 1990). The most compelling support for this function is the observation that loss of *Pou1f1* gene expression results in the combined loss of *Gh, Prl*, and *Tshb* gene expression in both mice (Camper et al., 1990; Li et al., 1990) and humans (Ohta et al., 1992; Radovick et al., 1992). Based on these data, we initiated our analysis of single cell transcriptomes with the assumption that the Pou1f1 lineages would be organized into three discrete clusters, defined by their mutually exclusive expression of *Gh, Prl,* and *Tshb* mRNAs.

We employed Drop-seq technology to assess this model of Pou1f1 lineage organization in an unbiased manner and to explore the full spectrum of pituitary cell composition (Macosko et al., 2015). Single cell transcriptome data were generated from 4 independent analyses, each of which contains a set of pituitaries harvested from 7 to 8-week old, sexually naïve female and male mice. After excluding cells of low sequencing complexity (see **Methods** and **Fig. S2**), the transcriptomes of 6,941 cells were retained for downstream analysis. Dimensionality reduction and clustering of the full set of 6,941 single cell transcriptomes was based on principal component analysis(Macosko et al.,

2015). Visualization of the data by *t*-distributed stochastic neighbor embedding (tSNE) (Hu et al., 2017; Macosko et al., 2015; Shekhar et al., 2016), revealed nine spatially distinct clusters surrounding a set of five closely juxtaposed clusters (**Fig. 1A)**.

The five centrally located cell clusters identified in the tSNE plot were noteworthy for their shared enrichment of *Pou1f1* mRNA. **(Fig. 1B and C**). The largest of these clusters was assigned as somatotropes (Som) based on the high level enrichment for both *Gh* and the cell surface receptor for the hypothalamic growth hormone releasing hormone (*Ghrhr*) (see violin and feature plots **Figs. 1B** and **C**)(Lin et al., 1993). The second Pou1f1^{+} cluster was identified as lactotropes (Lac) based on the high level expression of *Prl* mRNA (**Fig. 1C**) in conjunction with markers previously linked to *Prl* expression and lactotrope functions; glutamine receptors (*Gria2*, *Grik2*, and *Grik5*) involved in Prl hormone release (Durand et al., 2008), two transcriptional co-activators of estrogen receptor function (*Ddx5* and *Ddx17*) (Janknecht, 2010), and two transcription factors recently identified as enriched in *Prl*$^{+}$ cells and implicated in *Prl* gene activation (*Nr4a1* and *Nr4a2)* (**Table S1**) (Peel et al., 2018).

The transcriptome of a third Pou1f1^{+} cluster was closely aligned with the Lac cluster with the notable under-representation of *Prl* (Unk; **Fig. 1C**). This cluster did not match with any prior identified cell types in the mouse pituitary and was therefore assigned as Unknown (Unk). Dendrogram in Pou1f1^{+} clusters showed a strong concordance of the transcriptomes in the Lac and Unk clusters despite the absence of *Prl* in the latter (**Fig S3**). These results suggested that the Unknown cluster is composed of cells closely related to the lactotrope lineage.

The characteristics of a fourth major Pou1f1^{+} cluster could not be clearly linked to any of the currently defined pituitary cell lineages. This Pou1f1-enriched cluster ('Mult', as defined below) encompassed 17.5% of pituitary and was remarkable in several respects. First, the co-expression of *Gh* and *Prl* mRNAs was detected at robust levels that were in excess of those detected in the somatotrope (Som) and lactotrope (Lac) clusters. Secondly, the cells in this cluster were also highly enriched for mRNAs transcribed from the *POMC* gene at levels comparable to that detected in the 'Pou1f1-independent' melanotrope and corticotrope lineages (**Fig. 1B and C**)(Zhu et al., 2007). Thirdly, substantial number of cells in this third cluster also contained mRNAs encoding the gonadotrope hormone, *Lhb* (**Fig. 1B** and **C**). Lastly, a large fraction of the cells containing *Tshb* mRNA mapped to this cluster (**Fig. 1C** and **Fig. S4A**). On the basis of these observations, we provisionally assigned this cluster as a 'multi-hormone' producing cluster (Mult). 2D scatter plots, focusing on sets of pair-wise comparisons, confirmed that the great majority of cells in the Mult cluster were enriched for multiple hormone gene mRNAs (**Fig. S4**). In summary these data revealed a novel Pou1f1+ multi-hormone producing cluster that comprises a substantial fraction of the Pou1f1-dependent pituitary cell population.

The detection of a small cluster of cells that co-express *Pou1f1*$^{+}$ and proliferating cell markers such as Top2a and *Mki67* **(Fig. 1B**) is consistent with prior reports that the majority of proliferating cells in the adult pituitary are positive for *Pou1f1*expression (Cao et al., 2016; Zhu et al., 2015). In summary we observed in the single cell analysis of the adult pituitary an unexpected complexity of hormone gene expression and

identified a novel Pou1f1^{+} multi-hormone producing cluster that comprises a substantial fraction of the pituitary cell population.

Single cell RNA-seq identifies Pou1f1 independent hormone-producing cell lineages and non-hormonal cell clusters in the adult pituitary.

The nine remaining cell clusters that assembled on the tSNE plot lacked the high density of *Pou1f1* mRNA observed in the five central clusters (**Fig. 1B and C**). Three of these nine clusters could be directly assigned to specific hormone-expressing cell lineages based on patterns of marker gene expression (**Fig. 1B and C**). A cluster corresponding to melanotropes ('Mel') was assigned based on the co-expression of pro-opiomelanocortin (*POMC)* prohormone mRNA, the transcription factor Tbx19, and the melanotrope-restricted paired homeodomain transcription factor Pax7 (Budry et al., 2012; Mayran et al., 2018). A second cluster was assigned as a corticotrope cell cluster ('Cort'). These cells shared with the melanotrope cluster an enrichment for *POMC* and *Tbx19* mRNAs but absence of *Pax7* mRNA (Lamolet et al., 2001; Liu et al., 2006; Philips et al., 1997). A third *Pou1f1*-negative cluster was assigned to the gonadotrope lineage ('Gona' cluster) based on the enrichment for mRNAs encoding the two gonadotrope-specific hormone subunits, *Fshb* and *Lhb*, in conjunction with the gonadotrope-restricted cell surface receptor for the hypothalamic regulatory factor, *Gnrh* (Ingraham et al., 1994; Zhu et al., 2007). Thus the initial clustering analysis of the single cell transcriptomes from the adult mouse pituitary identified a set of Pou1f1-enriched clusters and clusters corresponding to three Pou1f1-independent lineages (melanotropes, corticotropes, and gonadotropes) (**Fig. 1A**).

The scRNA-seq data sets identified six clusters that represented non-hormonal cell lineages. Three of these clusters were identified as folliculostellate (FS) cells based on known marker genes (see below). FS cells have been proposed to serve a variety of structural, paracrine, and/or support functions in the pituitary (Le Tissier et al., 2012). Histologic identification of these cells has been based on an array of protein markers including *Anxa1*, *Vim*, *Mif*, and *S100* (Devnath and Inoue, 2008; Nakajima et al., 1980; Theogaraj et al., 2005) with variable expression levels of these markers pointing to the presence of sub-types of FS cells in the anterior pituitary (Allaerts and Vankelecom, 2005). The single-cell RNA-seq analysis organized FS cells into three distinct cell clusters ('FS1, 2, and 3' in **Fig. 1A and B**). FS3 is the major cluster with FS1 and FS2 containing far fewer cells. The three FS clusters accounted in aggregate for 8.2% of the total pituitary cell population, a number that is highly concordance with the relative composition (5~10%) of FS cells based on prior histologic studies (Devnath and Inoue, 2008). The FS1 cluster is unique among the three in containing mRNA for *Hes1*, a transcription factor required for normal pituitary development (**Table S1**). The markers for the other two FS cell clusters, FS2 and FS3, align with prior subcategorization of FS cell types as dendritic-like and astrocyte-like FS, respectively (Allaerts and Vankelecom, 2005). A separate cluster, lacking all hormone and FS markers, was assigned as microglia ('MG' cluster) based on the expression of the known MG marker genes, *Apoe* and *Ctss* (Guerreiro et al., 2012; Hu et al., 2017). The presence of this MG cluster in the single cell study supports a prior report of microglial cells in the anterior pituitary (Traverso et al., 1999). One additional non-endocrine cell cluster was assigned as a putative stem cell cluster ('$Sox2^{+}$' clusters; **Fig. 1A**) based on the shared expression of the progenitor/stem

markers *Sox2* (**Fig. 1B**). An erythrocyte cell cluster, most likely originating from blood within the pituitary, was defined by robust globin gene expression (BC cluster in **Fig. 1**) and is assumed to originate from blood in the dissected pituitaries. Therefore, these data reveal five cell clusters in the pituitary that serve functions other than direct production of polypeptide hormones.

In summary, the analysis of 6,941 single cell transcriptomes identifies eight hormone-expressing clusters, three clusters of folliculostellate cells, a set of putative stem cell clusters, and a single cluster of corresponding to a microglial cell population.

Single cell mRNA and protein analyses validate the prevalence of hormone co-expression.

The Drop-seq analysis revealed robust co-expression of *Gh* and *Prl* mRNAs in the Pou1f1^{+} multi-hormone (Mult) cluster and to a lesser extent in the adjacent Pouf1(+) Som, Lac, and MKi67 clusters (**Fig. 1**). Together these four clusters compose 64% of the analyzed pituitary cells. To explore this apparent co-expression of various hormone mRNAs, we carried out an initial orthogonal validation of *Gh*/*Prl* co-expression was carried out by single cell RNA fluorescent in situ hybridization (scRNA FISH). Primary pituitary cells isolated from 7-8 week old male mice (n = 986) were hybridized with arrays of fluorescent probes antisense to the *Prl* and *Gh* mRNAs (**Fig. 2A**). This analysis revealed that 61.6% of all the analyzed pituitary cells co-expressed *Prl* and *Gh* mRNAs (Gh^{+}/Prl^{+}) while 6.3% were uniquely positive for *Gh* mRNA (Gh^{+}/Prl^{-}) and none were uniquely positive for *Prl* mRNA expression (**Fig. 2B, left panel**). A parallel study of pituitary cells from female mice (n = 423) revealed 65.5% of the cells as dual positive

(*Gh*$^+$/*Prl*$^+$), 6.9% as uniquely *Gh* positive (*Gh*$^+$/*Prl*$^-$), and 16.5 % as uniquely *Prl* mRNA positive (*Prl*$^+$/*Gh*$^-$) (**Fig. 2B, right panel**). We conclude from these studies that co-expression *Gh* and *Prl* mRNAs is prevalent in the pituitary cell population.

To further explore the prevalent co-expression *Gh* and *Prl* genes, we next combined IF analyses of GH and PRL hormone proteins with scRNA FISH of the corresponding hormone mRNAs (**Fig. 3**). Analysis of 933 cells confirmed concordance of mRNA and protein expression from these two genes; all cells with *Gh* or *Prl* mRNA as visualized by scRNA FISH had a comparable IF signal for the corresponding protein (**Fig. 3**); when *Gh* or *Prl* mRNA was abundant the corresponding protein was abundant and when either mRNA was at trace levels or undetectable the corresponding protein was comparably trace or negative by IF (examples in **Fig. 3**). In no case did we observe a substantial discordance between corresponding IF and scRNA FISH signals. Consistent with Drop-seq analysis, these data support that *Gh* and *Prl* are co-expressed in majority of the Pou1f1$^+$ cells in the mouse adult pituitary.

The mapping of *Pomc* expression in the pituitary by Drop-seq revealed that *Pomc* mRNA was present at robust levels in the cells that constituted the multi-hormone cluster. The level of *Pomc* expression in the multi-hormone cluster was at levels equivalent to that detected in the melanotrope (*Pax7*$^+$ and *Tbx19*$^+$) and corticotrope (*Tbx19*$^+$ and *Crhr1*$^+$ but *Pax7*$^-$) lineages (**Fig. 1B** and **C**). The unexpected co-expression of high levels of *Pomc* mRNA with *Gh,* and *Prl* mRNAs in cells of the anterior pituitary was validated by scRNA FISH (**Fig. S5)**. Remarkably, 65% of all analyzed cells from male pituitary (n=466) (corresponding to 81% of the *POMC*-expressing cells) co-expressed both *Pomc* and *Gh* while only 15% of the cells (corresponding to 19% of the *Pomc* expressing cells)

were *Pomc*$^{+}$ but *Gh*$^{-}$ (**Fig. S5A**). A second scRNA FISH analysis in female pituitary cells (n=449) revealed that 74% of the cells co-expressed *Pomc* and *Prl* and only 6% of the cells were *Pomc*$^{+}$ but *Prl*$^{-}$ (**Fig. S5B**). These scRNA FISH studies are concordant with the initial Drop-seq data and lead us to conclude that the *Pomc* gene is co-expressed with the *Gh* and/or *Prl* gene(s) in majority of cells in the adult mouse pituitary.

Expression of *Tshb* is detected in the multi-hormone cluster rather than in a dedicated thyrotrope lineage.

Tshb is generally considered to constitute one of the three Pou1f1-dependent pituitary hormone genes (**Fig. S1**) and the expression of *Tshb* is thought to define a distinct POU1f1-dependent 'thyrotrope' lineage(Zhu et al., 2007). While the scRNA-seq analysis defined clusters corresponding to the Pou1f1-dependent somatotrope and lactotrope lineages, as well clusters corresponding to all three of the Pou1f1-independent lineages (corticotrope, melanotrope, and gonadotrope), the analysis failed to identify a discrete cell cluster that specifically corresponded to thyrotropes. Instead, *Tshb*+ cells were identified throughout the major 'Pou1f1 lineage' clusters with a substantial overlap with the multi-hormone cluster (**Fig. 1C**). A 3-dimensional scatter plot of *Tshb*, *Gh*, and *Prl* mRNA distributions revealed that 91.3% of *Tshb*$^{+}$ cells co-express *Gh* and/or *Prl* mRNAs **(Fig. 4A)**. This observation was validated by combining IF detection of TSHβ protein with scRNA FISH detection of *Gh* mRNA in male pituitaries (**Fig. 4B**); all cells positive for TSHβ by IF (a total of 141 cells examined) were also positive for *Gh* mRNA by scRNA FISH with the majority of these cells expressing *Gh* mRNA at very high levels (**Fig. 4C**). A series of pair-wise comparisons supported this observation by demonstrating

that a majority of cells positive for *Tshb* mRNA were also positive for either *Prl* or *Gh* mRNAs (**Fig. S4**) and in most cases all three hormones were co-expressed in the same cell (**Fig. 4A)**. These orthogonal studies lead us conclude that *Tshb* expression, while demonstrating the expected localization to Pou1f1+ cells, does not define a distinct 'thyrotrope' cell cluster. Instead, we find that *Tshb* is expressed in conjunction with *Gh* and/or *Prl*, and maps predominantly to the multi-hormone cluster.

Sexual dimorphism in the organization and composition in the mouse pituitary

Synthesis and secretion of the pituitary hormones are impacted by multiple gender specific developmental and physiologic stimuli. These controls drive critical somatic alterations linked to puberty, reproductive cycling, pregnancy, and lactation. The degree to which these gender specific functions are linked to differences in the cellular composition of the male and female pituitaries remains poorly defined (Lamberts and Macleod, 1990; Nishida et al., 2005). To address the issue at the single-cell level we compared the transcriptomes of cells isolated from male and female pituitaries in our Drop-seq data set (**Figs. S2D** and **5A).** Gender-specific analysis of major *Pou1f1*$^{+}$ clusters revealed a relative predominance of somatotropes over lactotropes in males with a reciprocal enrichment of lactotropes over somatotropes in females (**Fig. 5B**). Of particular note, the lactotrope-related (Unk) cluster was more dominant in the females (**Fig. 5B**). Marked sexual dimorphism was also evident in the gonadotrope cluster; this cluster constituted a substantially larger fraction of the pituitary cell population in male than female mice (5.1% vs 1.6% of total pituitary cells, respectively) (**Fig. 5A and B**). This dimorphism in gonadotrope cluster size is consistent with previously-reported higher

levels of Fshβ in the blood of male verses female mice (Michael et al., 1980). In contrast *Lhb* expression was equivalent between males and females and was predominantly expressed in the multi-hormone cluster in both sexes (**Fig. 5A**). These data led us to conclude that relative representations of somatotropes and lactotropes populations differ between the two genders and that the two gonadotrope hormones, *Lhb* and *Fshb*, are differentially expressed in the male and female pituitaries both quantitatively and with relation to cell clustering.

The response of hormone expressing clusters to major physiologic demands

We next sought validate and extend our analyses of pituitary cell populations to settings of defined physiologic stress. One of the most dramatic alterations in pituitary hormone production is the 10-15 fold increase in PRL levels in the blood of lactating females, both mouse and human (Le Tissier et al., 2015). The basis for this increase in serum PRL has remained open to question (Castrique et al., 2010). In particular, it remains unclear to what extent this increase reflects an expansion of the lactotrope lineage and/or to alterations in hormone gene expression per lactotrope. To address this issue, we compared the pituitary cell-type composition in three 13 week-old lactating female mice 2 weeks into lactation (**Fig. 6**) in two independent experiments (Rep 1 (one mouse) and Rep 2 (two mice)) with an age-matched virgin female control. This analysis revealed several noteworthy observations. First, the overall pattern of cell clustering in these 13 week old females was highly similar to that of 7-8 week old male and female mice. Of particular note was the formation of a multi-hormone cluster in both studies (compare **Figs. 6A** and **1A**). Second, the comparison of the virgin female with the age

matched lactating females revealed an expansion of the lactotrope cluster in the lactating state (33.6% in control to 43.2% in lactating mice) with reciprocal decreases in representation of clusters representing gonadotropes, corticotropes, and Sox2+ cells (**Fig. 6B**). Of note, however, was the absence of an appreciable difference in the representation of somatotropes in the pituitaries from the lactating *vs* control mice (**Fig. 6B**). These data lead us to conclude that there are substantial shifts in specific pituitary cell populations in the transition to the lactating state with a net increase in the representation of lactotropes.

The question of how lactation impacts *Prl* production was further explored by a focused analysis on the lactotrope transcriptomes. We performed PCA analysis on 4,435 lactotrope cells (3,383 from lactating mice and 1,052 cells from age-matched control mice). PCA analysis separated cells into two partially overlapping cohorts ordered by physiologic states (control and lactating) indicating a transcriptional transition required by the physiological demands along the PC1 (**Fig. S6** and **Fig. 6C**). The level of *Prl* mRNA was significantly higher in cells within the lactotrope cohort of cells originating from the lactating mice (adjusted *p*-value $=1.06\text{x}10^{-30}$) (**Fig. 6D**). This higher level of *Prl* mRNA levels in the lactotropes of the lactating mice was paralleled by an increase in expression of the neuroendocrine vesicle secretory protein *Chgb* (Barbosa et al., 1991; Gill et al., 1991) (adjusted *p*-value $=2.19\text{x}10^{-26}$) (**Fig. 6E**). The increase in *Chgb* is consistent with the high demand for PRL secretion during lactation. Therefore, the enhancement of PRL production during lactation are likely caused by both the increased number of lactotropes as well as an elevation in *Prl* gene expression within the lactotrope cells.

In addition to its expression in lactotropes, *Prl* expression is also a prominent

attribute of the multi-hormone cell cluster (**Figs. 1 and 6F**). For this reason, we next sought to determine whether the cells in the multi-hormone cluster contributed to the increased pituitary production of Prl in support of lactation. While the representation of the multi-hormone cluster in the lactating mice did not differ appreciably from that in the control (12.1% vs 10.1%, respectively) (**Fig. 6B**), there was a significant increase in the expression of *Prl* (adjusted *p*-value = 1.51×10^{-11}) and *Nr4a2* mRNAs in the cells within the cells in this cluster (adjusted *p*-value =1.56×10^{-5}) (**Fig. 6F**). Nr4a2 is an orphan nuclear receptor transcription factor that has recently been reported to bind to, and enhance the activity of, the *Prl* promoter (Peel et al., 2018). Increased expression in *Prl* and *Nr4a2* was associated with reciprocal decreases in the expression of *Gh* and *Lhb* mRNAs (adjusted *p*-value =2.68×10^{-7} and 1.24×10^{-11}, respectively) (**Fig 6F)**. We also observed a significant increase of *Prl* expression (adjusted *p*-value = 6.92×10^{-37}) in the somatotropes of lactating mice compared with the control (**Fig. 6F**). In summary, these results demonstrated that the cells in the multi-hormone and somatotrope clusters, while not demonstrating in noticeable shift in relative composition during lactation, undergo transcriptomic shifts that support increased production of PRL in the lactating female. These findings lead us to conclude that the induction of Prl expression in lactating females is associated with a combination of shifts in cell composition with shifts in transcriptome profiles in the pituitary.

We next assessed the impact of human *growth hormone releasing hormone* (*hGhrh*) on cell composition and function of the pituitary. Ghrh is the major hypothalamic regulator of somatotrope function(Mayo et al., 1988). This factor is delivered to the anterior pituitary *via* a local venous portal circuit and binds to a surface

receptor (Ghrhr) on somatotropes. The Ghrhr-triggered signaling pathway stimulates the proliferation of somatotropes as well as GH synthesis and secretion (Gaylinn, 2002; Mayo et al., 2000). The mt/hGhrh transgenic model used for this study has been previously shown to drive high levels of GH expression in the mouse with resultant gigantism (Ho et al., 2002; Mayo et al., 1988). Drop-seq analysis was carried out on 2,842 pituitary cells isolated from two 8-week old virgin female mice carrying a highly expressed *mt/hGhrh* transgene (Mayo et al., 1988) compared with age-matched virgin non-transgenic females. Single-cell transcriptomic analysis revealed the assembly of an array of clusters that paralleled those detected in 8 week old non-transgenic mice as well as the 13 week old virgin and lactating females (**Fig. 7A** c/w **Figs. 1** and **6**). A Multi-hormonal cluster was again observed in this analysis as well as the full array of hormone-expressing and non-hormonal cell clusters see in the preceding analyses. Comparison of the *hGhrh* pituitaries and the WT revealed the presence of a markedly expanded somatotrope cluster (from 22.3% to 41.7%) (**Fig. 7B**). While there was no significant change in the level of *Gh* mRNA in the individual somatotropes, there was a significant decrease in the levels of *POMC* and *Prl* mRNAs in these cells (**Fig. 7C**). The increase in the size of the somatotrope cluster was paralleled by a reciprocal decrease in the sizes of the multi-hormone cluster (from 18.0% to 12.1%) (**Fig. 7B**) as well the FS and $POMC^{+}$ clusters (**Fig. 7B**). Differential gene expression analysis of lactotropes in the *hGhrh*-transgenic pituitaries revealed significant increases in *Gh* mRNA while the overall size of the lactotrope cluster was not appreciably altered. Importantly, significant decreases in the expression of the *Prl*, *Lhb*, and *POMC* mRNA were detected in the multi-hormone cells while *Gh* expression was unchanged (**Fig. 7C**). These changes in cell cluster

representation and gene expression in response to *Ghrh* overexpression highlight the contributions and coordination of the three major Po1f1-expressing cell clusters in both their relative cell representations and in their gene expression profiles. These studies further validated the utility of scRNA-seq analysis in identifying shifts in cell representation and transcriptome expression profiles in response to physiologic demands.

Discussion

Current understanding of pituitary function is based upon a binary model in which each of the six distinct endocrine cell types is dedicated to the synthesis and secretion of its corresponding polypeptide hormone (**Fig. S1**). The function of each lineage is considered as mutually-exclusive and under the control of a corresponding set of discrete hypothalamic/pituitary regulatory circuits (Davis et al., 2013; Kelberman et al., 2009; Zhu et al., 2007). However, scattered reports of pituitary cells co-expressing multiple hormones have suggested that the organization and function of the pituitary may be more complex than commonly appreciated (Childs, 2000; Frawley and Boockfor, 1991; Seuntjens et al., 2002a; Villalobos et al., 2004b) and the prevalence and complexity of 'multi-hormone' cells in the adult anterior pituitary has remained undefined on a systematic and global level. Thus, understanding the compositions and functions of pituitary cell lineages and their relationships to hormone expression warrants further study.

Here we report a series of orthogonal single-cell analyses that address fundamental aspects of pituitary cell organization, lineage specification, and functional plasticity. Our single cell transcriptome analysis yielded findings that were consistent

with certain aspects of existing models while substantially extending and modifying others. While the analysis confirmed the presence of three discretely clustering *Pou1f1*-independent cell lineages (corticotropes, melanotropes, and gonadotropes (**Fig. 1A)**), it reveals that the organization and functions of the Pou1f1-dependent lineages are substantially complex (**Fig. 1**). The initial presumption going into this study was that the clustering analysis would generate three *Pou1f1*$^{+}$ clusters corresponding to somatotropes, lactotropes, and thyrotropes, each dedicated to the exclusive expression of its corresponding hormone; *Gh, Prl,* and *Tshb*, respectively (**Fig. S1**) (Zhu et al., 2007). However, our unbiased scRNA-seq failed to confirm the existence of a unique 'thyrotrope' lineage and revealed that the majority of *Tshb* mRNA expression, along with a significant fraction of *Gh* and *Prl* mRNAs, were derived from a novel Pou1f1-expressing 'multi-hormonal' cell cluster. The discovery of this substantial multi-hormone cell cluster challenges current models of pituitary lineage distinctions and the segregation of hormone expression.

Analysis of the multi-hormonal cell cluster revealed that it constitutes a substantial fraction (17.5%) of total pituitary cell population under homeostatic conditions. Our multiple independent scRNA-seq analyses on pituitaries isolated from mice of varying ages and genders as well as under two well defined setting of physiologic stress reproducibly identified this unique multi-hormone cluster (**Figs, 2, 6, and 10**). Most intriguing was the observation that the cells in this cluster not only expressed well defined Pou1f1-dependent genes such as *Gh*, *Prl*, and *Tshb*, but also expressed robust levels of mRNAs encoded by two genes, *Pomc* and *Lhb*, that as traditionally categorized as Pou1f1-independent. A series of scatter plots and single cell RNA and protein

imaging studies documented co-expression of the 'Pou1f1-dependent' and the 'Pou1f1-independent' hormone genes within individual cells (**Figs. 2, S4,** and **S5**). Collectively, these results indicate that the novel 'Multi-hormone lineage' cell cluster is present in pituitary independent of age, gender, and physiologic stresses and represents a potential source of hormone gene expression.

While multi-hormone producing cells have been previously identified by others using immuno-fluorescent and targeted RT-PCR analyses (Seuntjens et al., 2002a; Seuntjens et al., 2002b; Villalobos et al., 2004a), their abundance, array of hormone gene expression, and physiological function(s) have remained unclear. Our analyses reveal that the cells in this Multi-hormone cluster respond to physiological demands *in vivo*. For example, in lactating females, the level of *Prl* expression increases in the cells in this cluster with reciprocal decreases in *Lhb* and *Gh* mRNAs. Likewise, in transgenic mice overexpressing the *hGhrh* gene, *Gh* expression increases in the multi-hormone cells while the expression of other pituitary hormones significantly decrease. These observations suggest that cells in the multi-hormone cluster are able to respond to substantial physiological demands and exhibit plasticity of pituitary function and hormone production.

The developmental origin(s) of the *Pou1f1*$^{+}$ multi-hormonal cells in adult mouse pituitary is presently unclear. The broad functional capacity of these cells cannot be accounted for in current models of anterior pituitary development and cellular differentiation (**Fig. S1**). However, recent studies suggest that these cells may be induced by the actions of the specific transcription factors including *Prop1*. *Prop1*, a paired-like homeodomain transcription factor, was initially described as a factor that triggers the

activation of *Pou1f1* and the differentiation of the Pou1f1-dependent lineages during pituitary development (Andersen et al., 1995; Gage et al., 1996). However, recent lineage tracing studies in the mouse reveal that Prop1 is in fact expressed in progenitor cells that generate the full spectrum of endocrine cell types in the pituitary, those considered to be 'Pou1f1-dependent' as well as those considered to be 'Pou1f1-independent' (Davis et al., 2016; Perez Millan et al., 2016). Multi-hormone expressing cells may therefore be generated through the activity of Prop1 during pituitary development, and may serve as a transitional cell pool that can respond to shifts in hormone production in response to physiological demands such as pregnancy, lactation, and pubertal growth.

In addition to revealing the presence of the multi-hormone cell cluster, the Drop-seq analysis highlighted complex relationships between the functions of the two other major Pou1f1 clusters, the somatotropes and lactotropes. While the cells in these two clusters could be readily identified by a preponderant expression of either *Gh* or *Prl* as well as by a number of corresponding signatory mRNAs (see **Fig, 1** and accompanying text), the majority of these cells co-expressed *Gh* and *Prl* to varying degrees (**Fig. 1** and **Fig. 2**). Furthermore, the levels of *Prl* expression in somatotropes increased substantially in lactating mice while *Gh* expression increased significantly in the lactotropes of the *hGhrh* transgenic mice (**Fig. 6 and 7**). These data suggest that the capacity of the somatotrope and lactotrope lineages to express both *Prl* and *Gh* may be critical to a robust response to major physiological demands.

The Drop-seq analysis identified a population of $Sox2^{+}$ cells that we have provisionally categorized as a stem/progenitor cell cluster ($Sox2^{+}$ cluster; **Fig. 1**). The designation of this cluster is consistent with prior reports of a stem cell population in the

adult mouse pituitary (Chen et al., 2006; Fauquier et al., 2008) that is postulated to support expansion of pituitary synthetic capacity (Willems et al., 2016). *In vitro* studies reveal that these stem cells are capable of differentiating to hormone producing cells (Fauquier et al., 2008; Gleiberman et al., 2008). The cells in the *Sox2*$^{+}$ cluster appear to be mitotically quiescent as indicated by the lack the proliferating cell marker, Mki67 (Scholzen and Gerdes, 2000). It will be interesting to explore in subsequent studies whether the decrease of Sox2+ cells in the pituitary of lactating mouse (**Fig. 6**) can be functionally linked to the increase in the representation of the lactotrope cell cluster during lactation.

The hypothalamic signaling protein, Ghrh, binds to the Ghrh receptor (Ghrhr) on the surface of somatotropes in the pituitary and this interaction stimulates the expansion of the somatotrope population and induction of *Gh* expression (Gaylinn, 2002). Our scRNA-seq analysis of primary pituitary cells from mice overexpressing the hypothalamic factor hGhrh (*mt/hGhrh* transgenic mice) reveals a marked expansion in the somatotrope lineage in conjunction with shifts in re transcriptome profiles of hormone producing cells (multi-hormone cells and *Pomc*+ cells) as well as non-hormone producing FS cells (**Fig. 7**). The response of FS cell population in this setting may relate to the putative stem cell function of FS cells (Inoue et al., 2002). Future lineage tracing studies that further explore the lineage shifting in the pituitary of *hGhrh* transgenic mouse will be of interest.

The synthesis and secretion of the pituitary hormones are impacted by multiple physiologic variables that directly relate to sexual maturation, reproduction, and somatic development. As such, sexual dimorphism in pituitary structure and hormonal output has

been previously identified in a number of these settings (Lamberts and Macleod, 1990; Michael et al., 1980; Nishida et al., 2005). Of interest, the Drop-seq analysis of the pituitaries of 7-8 week old, sexually-naïve mice confirmed that even at the young adult stage there is strong evidence for sexual dimorphism. The most striking gender distinctions in this regard was the dominance of the somatotropes in the males (**Fig. 5**), the overall enrichment of lactotropes in in females (**Fig. 5**), and the distinct patterns of gonadotrope hormone expression between the two genders (**Fig. 5**).

The characterization of cell clusters identified in the analysis of scRNA-seq data sets was accomplished using an array of previously defined markers of cell function and hormone expression (Chen et al., 2017; Hu et al., 2017; Macosko et al., 2015; Shekhar et al., 2016). This approach can now be further extended to identify additional factors involved in the differentiation and/or maintenance of pituitary cell populations and functions. While genetic approaches have been successful in identifying a number of key regulators of pituitary development and cellular differentiation (Brinkmeier et al., 2009; Zhu et al., 2007), many of these factors are not cell type restricted and as such, are likely to work in conjunction with additional, as yet undefined, signaling molecules and transcriptional regulators to direct patterns of hormone expression. Applying unsupervised searches is likely to reveal subsets of relevant factors. As an example, the increase of *Prl* expression is associated with the increase of Nr4a2 expression in multi-hormone cluster (**Fig. 6**). The observation is consistent with our recent report that Nr4a2 functions as an activator for *Prl* expression (Peel et al., 2018). Therefore, searching for additional lineage-enriched transcription factors and signaling molecules can now be extended, validated, and functionally tested in subsequent studies.

In conclusion, we have applied complementary single-cell RNA sequencing and imaging-based analyses to analyze the transcriptomes of cells in the adult mouse pituitary. The results have revealed unanticipated levels of cellular diversity and lineage plasticity in pituitary cell-type composition and hormone expression. The findings reveal prominence of cells that co-express multiple hormones, sexual dimorphisms of lineage composition and cell prevalence, and the plasticity of cell functions in response to major physiologic demands. These single-cell transcriptomic data sets, along with experimental approaches to identifying the factors that underlie these complexities of lineage structure and function, can now be further extended to explore pituitary functions in settings of physiologic stress and disease.

Methods

Animals

Six week old CD1 mice were purchased from Charles River (Wilmington, MA) and were housed for 1 to 2 weeks in rooms with 12-hour light/dark cycles prior to studies. All aspects of the mouse studies were reviewed and approved by the University of Pennsylvania Laboratory Animal Use and Care Committee. The *mt/hGRF* transgenic mice were originally obtained from Dr. Ralph Brinster at the University of Pennsylvania (Hammer et al., 1985) and have been described in a number of our prior reports (Ho et al., 2002; Ho et al., 2008).

Single cell preparation for Drop-seq

Single cell pituitary suspensions were prepared by non-enzymatic methods as previously descripted (Ho et al., 2011) with minor modifications to adapt to the Drop-seq protocol (Macosko et al., 2015). Briefly, the pituitaries were isolated and washed with cold PBS, incubated with 1 ml of enzyme-free cell dissociation buffer (Life technologies, Carlsbad, CA) for 1 minute, passed through a 40 μm cell strainer, and then re-suspend in 10 ml of PBS. The cells were diluted to 100 cells/μl in PBS with 0.01% BSA prior to the capture of the cells

Single-cell RNA-Seq library preparation and sequencing

Drop-seq was performed as previously described with minor modifications (Macosko et al., 2015). Specifically, cells were captured on barcoded beads, reverse transcribed, and treated with exonuclease prior to amplification. The cDNA from an aliquot of 6,000 beads was amplified by PCR in a volume of 50 μL (25 μL of 2x KAPA HiFi hotstart readymix (KAPA biosystems), 0.4 μL of 100 μM TSO-PCR primer (AAGCAGTGGTATCAACGCAGAGT), 24.6 μL of nuclease-free water) to determine an optimal number of PCR cycles for cDNA amplification. The thermal cycling parameter was set to: 95°C for 3 min; 4 cycles of 98°C for 20 sec, 65°C for 45 sec, 72°C for 3 min; 9 cycles of 98°C for 20 sec, 67°C for 45 sec, 72°C for 3 min; 72°C for 5 min, hold at 4°C. Then amplified cDNA was purified twice with 0.6x SPRISelect beads (Beckman Coulter) and eluted with 10 μL of water. 10% of amplified cDNA was used to perform real-time PCR analysis (1 μL of purified cDNA, 0.2 μL of 25 μM TSO-PCR primer, 5 μL of 2x KAPA FAST qPCR readymix, and 3.8 μL of water) to determine the additional number of PCR cycles needed for optimal cDNA amplification (Applied

Biosystems QuantStudio 7 Flex). PCR reactions were then optimized per total number of barcoded beads collected for each Drop-seq run, adding 6,000 beads per PCR tube, and run according to the aforementioned program to enrich the cDNA for 4 + 12 to 13 cycles. The amplified cDNA was 'tagmented' using the Nextera XT DNA sample preparation kit (Illumina, cat# FC-131-1096), starting with 550 pg of cDNA pooled in equal amounts from all PCR reactions for a given run. After quality control analysis using a Bioanalyzer (Agilent), libraries were sequenced on an Illumina NextSeq 500 instrument using the 75-cycle High Output v2 Kit (Illumina). The library was loaded at 2.0 pM and the Custom Read1 Primer (GCCTGTCCGCGGAAGCAGTGGTATCAACGCAGAGTAC) was added at 0.3 μM in position 7 of the reagent cartridge. The sequencing configuration was 20 bp (Read1), 8 bp (Index1), and 50 or 60 bp (Read2). In total, 8 mouse pituitary samples, including 4 replicates of male and 4 replicates of female, were analyzed with Drop-seq in five sequencing runs.

Read mapping

Paired-end sequencing reads of Drop-seq were processed as previous described (Hu et al.). Briefly, after mapping the reads to the mouse genome (mm10, Gencode release vM13), exonic reads mapped to the predicted strands of annotated genes were retrieved for the cell type classification. Uniquely mapped reads were grouped by cell barcode. To digitally count gene transcripts, a list of UMIs in each gene, within each cell, was assembled, and UMIs within ED = 1 were merged together. The total number of unique UMI sequences was counted, and this number was reported as the number of

transcripts of that gene for a given cell. Raw digital expression matrices were generated for the 5 sequencing runs.

Background correction of the cell transcriptomes

The raw digital expression matrices were combined and loaded into the R package Seurat (v 2.0.1) (Butler and Satija, 2017). Only genes found to be expressing in >10 cells were retained. Cells with a relatively high percentage of UMIs mapped to mitochondrial genes (> 0.1) were discarded. Considering the unique characterize of pituitary cells, with *Gh* mRNA comprising > 30% of transcripts in many cells, the libraries were predicted to be of relatively low-complexity. For this reason, the cut-off for the minimal number of detected genes (nGene) was set at nGene > 100, nGene < 4000 and nUMI > 300. Cell cycle effect was accessed by the function "*CellCycleScoring*" in Seurat. The level of expressed genes in the cell was scaled and centered along each gene. For initial assessment of single cell RNA-seq data, we perform clustering with the following parameters setting (*y.cut.off*=0.6 in *FindVariableGenes* function, *dims.use* =1:20 and *resolution*=0.6 in *FindClusters* function). All other parameters in the analysis were set as default. After initial clustering, highly transcribed hormone genes (*Gh*, *Prl* and *Pomc*) could be detected in blood cells (**Fig. S2**), most likely representing cross-contamination of free RNAs. Since these mRNAs are highly expressed in the pituitary but should be absent in the blood cells, their levels in blood cells represent a background noise signals. We adapted a previous background correction approach (Han et al., 2018) to correct the expression level of contaminated mRNA. We assumed that the cell barcodes with less than 100 UMI or 100 nGene correspond to the empty beads exposed to free RNA during

the cell dissociation or droplet breakage steps. The average of nUMI for the cell barcodes (< 100 Gene or < 100 UMI) was therefore calculated and used to perform a background correction by subtracting this value from the raw nUMI digital expression matrix, and the negative value was then set to zero. After correction, UMI counts for all cells were scaled by total UMI counts, multiplied by 10,000, and transformed to log space. A final set of 6,995 cells was obtained for subsequent analysis.

PCA analysis and Clustering

The highly variable genes were identified using the function *FindVariableGenes* with the parameters: *x.low.cutoff = 0.05and y.cutoff = 0.6* in Seurat, resulting in 2,724 highly variable genes. When PCA analysis was run on those highly variable genes, we found that 4th top PC (explained 3.45 variation) was split on immediate early genes (IEGs; Junb, Fos and Egr1), that were most likely induced by whole cell dissociation process. To regress out the contribution from IEGs, we assign each cell a IEG score using averaged normalized expression levels (log2(TPM+1)) of the IEG gene set (**Fig. S2**). We factored in a list of 172 IEGs as previously defined by others (Tyssowski et al., 2018). Cell cycle and dissociation effects were regressed out using the function *ScaleData* in Seurat. The expression level of expressed genes in the cell was scaled and centered along each gene.

The top 20 PCs, which explained more variability than expected by chance using a permutation-based test as implemented in Seurat, were selected and used for two-dimension t-distributed stochastic neighbor embedding (tSNE), with the default parameters. Additionally, we tried different number of PCs for clustering and found that

the variation of PC number selection is relatively insensitive to the clustering results (**Fig. S2**). Cells were classified into 14-23 clusters with the resolution parameter from 0.6 to 2. Additionally, a classification hierarchy of clusters was built by implemented function "*BuildClusterTree*" in Seurat and a random forest classifier algorithm was used to examine cluster distinctness. Clusters with higher than 0.1 Out-of-bag error (OOBE) from a random forest classifier were merged. Clustering resolution parameters could be varied quantitatively based on the number of cells being clustered. After the clustering results with different resolutions were compared and evaluated, we used a resolution value of 0.6 and were able to assign 6,995 nuclei into 14 clusters.

Identification of Differentially Expressed Genes

Differential gene expression analysis between control and transgenic or lactation hormone clusters was performed using the function *FindMarkers* in Seurat, using a Wilcoxon rank sum test. Genes with an adjust *P*-value less than 0.05 were considered to be differentially expressed.

Probe design for single-cell RNA fluorescent *in situ* hybridization (scRNA FISH)

The strategy for the scRNA FISH probe design followed the strategy for the Single- molecule Oligopaint FISH (Beliveau et al., 2015). Two sets of oligo probes were used to detect each mRNA species. The 40 nt primary probes contained 20 nt complementary to the exons of the mRNAs (*Gh*, *Prl*, and *POMC)* with a 20 nt non-genomic tag located at the 5' end. 19 to 21 probes were used in each probe library. The sequences of the tag were unique for each mRNA library (Beliveau et al., 2015). A

fluorophore-labeled secondary oligo with base complementarity to the sequences of the tag was used to detect the mRNA molecules. All oligos were synthesized by Integrated DNA Technologies (IDT; Coralville, IA). The sequences of the primary and secondary oligos are available upon request.

scRNA FISH and immuno-fluorescent-scRNA (IF-scRNA) FISH

The procedures for RNA FISH followed were as described (Beliveau et al., 2015; Ho et al., 2013; Ragoczy et al., 2006) with modification. Briefly, single cell suspensions were prepared as described in the Drop-seq protocol and loaded onto poly-lysine coated slides (Ho et al., 2013). The cells were fixed with 3.7% formaldehyde and washed with PBS. The slides were treated with 70% EtOH at 4°C for overnight. 50 pmol of primary oligo library (19 to 22 oligos) and equal amount of fluorophore-labeled secondary were used for each slide. Prior to hybridization, the slides were washed with PBS and sequentially dehydrated in 70%, 90%, and 100% ETOH. The slides were equilibrated in 25% formamide/2X SSC, pH 7.0. The mixture of the primary oligo probes and the secondary probes were hybridized to the cells in 25% formamide/10% dextran sulfate/2XSSC/5 mM ribonucleotide vanadate complex/0.05% BSA/1μg/μl *E.coli* tRNA. The probes were heat denatured at 80°C for 5 min., pre-annealed at 37°C and then hybridized overnight at 37°C in a humidified chamber. Slides were washed in 25% formamide/2X SSC, pH 7 and washed in 2X SSC at 37°C. The slides were equilibrated in 0.1M Tris-HCl, pH 7.5/0.15 M NaCl/0.05% Tween 20 at room temperature for IF-scRNA FISH studies or mounted with Fluoroshield with DAPI (Sigma, St. Louis, MO).

For the IF-scRNA FISH, the slides were blocked in 145 mM NaCl /0.1M Tris pH 7.5/2% BSA/2 mM ribonucleotide vanadate complex. Gh was detected using monkey anti-rat GH that cross-reacts with mGh and PRL was detected using rabbit anti-mouse PRL (National Hormone and Peptide Program, NIH) as described (Ho et al., 2013). The secondary antibody used to detect Gh was a fluorophore-conjugated donkey anti-human IgG and the secondary antibody used to detect PRL was fluorophore-conjugated donkey anti-rabbit IgG (Jackson immnoResearch Inc). The slides were mounted as for the scRNA FISH.

Image Analysis

Image capture were collected on an Olympus IX70 inverted microscopy using a cooled CCD camera and de-convoluted using the Deltavision Softworx software (Applied Precision, WA) as described ((Ho et al., 2013). The images were analyzed using ImageJ software (NIH).

Acknowledgments

We thank Dr. Sonny Nguyen for suggestions on the scRNA FISH. We are grateful to Dr. Andrea Stout of the Microscopy Core in the Department of Cell and Development Biology, Perelman School of Medicine, University of Pennsylvania. This work was supported by National Institutes of Health (NIH) Grants DK107453 (to S.L and Y.H) and R00HG007982, DP2HL142044 and a University of Pennsylvania Epigenetics Institute Pilot Grant (to H.W).

Author Contributions

Y.H., H.W., and S.A.L designed experiments. Y.H., P.H., and M.P. conducted the experiments. P.H., H.W., and P.G-C performed the bioinformatic analyses. Y.H., P.H., H.W., and S.A.L wrote the manuscript. All authors read and approved the manuscript.

Declaration of Interests

The authors declare no competing financial interests.

References

Allaerts, W., and Vankelecom, H. (2005). History and perspectives of pituitary folliculo-stellate cell research. Eur J Endocrinol *153*, 1-12.

Andersen, B., Pearse, R.V., 2nd, Jenne, K., Sornson, M., Lin, S.C., Bartke, A., and Rosenfeld, M.G. (1995). The Ames dwarf gene is required for Pit-1 gene activation. Dev Biol *172*, 495-503.

Barbosa, J.A., Gill, B.M., Takiyyuddin, M.A., and O'Connor, D.T. (1991). Chromogranin A: posttranslational modifications in secretory granules. Endocrinology *128*, 174-190.

Beliveau, B.J., Boettiger, A.N., Avendano, M.S., Jungmann, R., McCole, R.B., Joyce, E.F., Kim-Kiselak, C., Bantignies, F., Fonseka, C.Y., Erceg, J.*, et al.* (2015). Single-molecule super-resolution imaging of chromosomes and in situ haplotype visualization using Oligopaint FISH probes. Nat Commun *6*, 7147.

Brinkmeier, M.L., Davis, S.W., Carninci, P., MacDonald, J.W., Kawai, J., Ghosh, D., Hayashizaki, Y., Lyons, R.H., and Camper, S.A. (2009). Discovery of transcriptional regulators and signaling pathways in the developing pituitary gland by bioinformatic and genomic approaches. Genomics *93*, 449-460.

Budry, L., Balsalobre, A., Gauthier, Y., Khetchoumian, K., L'Honore, A., Vallette, S., Brue, T., Figarella-Branger, D., Meij, B., and Drouin, J. (2012). The selector gene Pax7 dictates alternate pituitary cell fates through its pioneer action on chromatin remodeling. Genes Dev *26*, 2299-2310.

Butler, A., and Satija, R. (2017). Integrated analysis of single cell transcriptomic data across conditions, technologies, and species. bioRxiv.

Campbell, J.N., Macosko, E.Z., Fenselau, H., Pers, T.H., Lyubetskaya, A., Tenen, D., Goldman, M., Verstegen, A.M., Resch, J.M., McCarroll, S.A.*, et al.* (2017). A molecular census of arcuate hypothalamus and median eminence cell types. Nat Neurosci *20*, 484-496.

Camper, S.A., Saunders, T.L., Katz, R.W., and Reeves, R.H. (1990). The Pit-1 transcription factor gene is a candidate for the murine Snell dwarf mutation. Genomics *8*, 586-590.

Cao, D., Ma, X., Cai, J., Luan, J., Liu, A.J., Yang, R., Cao, Y., Zhu, X., Zhang, H., Chen, Y.X.*, et al.* (2016). ZBTB20 is required for anterior pituitary development and lactotrope specification. Nat Commun *7*, 11121.

Castrique, E., Fernandez-Fuente, M., Le Tissier, P., Herman, A., and Levy, A. (2010). Use of a prolactin-Cre/ROSA-YFP transgenic mouse provides no evidence for lactotroph transdifferentiation after weaning, or increase in lactotroph/somatotroph proportion in lactation. J Endocrinol *205*, 49-60.

Chen, J., Crabbe, A., Van Duppen, V., and Vankelecom, H. (2006). The notch signaling system is present in the postnatal pituitary: marked expression and regulatory activity in the newly discovered side population. Mol Endocrinol *20*, 3293-3307.

Chen, R., Wu, X., Jiang, L., and Zhang, Y. (2017). Single-Cell RNA-Seq Reveals Hypothalamic Cell Diversity. Cell Rep *18*, 3227-3241.

Childs, G.V. (2000). Green fluorescent proteins light the way to a better understanding of the function and regulation of specific anterior pituitary cells. Endocrinology *141*, 4331-4333.

Davis, S.W., Ellsworth, B.S., Perez Millan, M.I., Gergics, P., Schade, V., Foyouzi, N., Brinkmeier, M.L., Mortensen, A.H., and Camper, S.A. (2013). Pituitary gland development and disease: from stem cell to hormone production. Curr Top Dev Biol *106*, 1-47.
Davis, S.W., Keisler, J.L., Perez-Millan, M.I., Schade, V., and Camper, S.A. (2016). All Hormone-Producing Cell Types of the Pituitary Intermediate and Anterior Lobes Derive From Prop1-Expressing Progenitors. Endocrinology *157*, 1385-1396.
Devnath, S., and Inoue, K. (2008). An insight to pituitary folliculo-stellate cells. J Neuroendocrinol *20*, 687-691.
Durand, D., Pampillo, M., Caruso, C., and Lasaga, M. (2008). Role of metabotropic glutamate receptors in the control of neuroendocrine function. Neuropharmacology *55*, 577-583.
Fauquier, T., Rizzoti, K., Dattani, M., Lovell-Badge, R., and Robinson, I.C. (2008). SOX2-expressing progenitor cells generate all of the major cell types in the adult mouse pituitary gland. Proc Natl Acad Sci U S A *105*, 2907-2912.
Frawley, L.S., and Boockfor, F.R. (1991). Mammosomatotropes: presence and functions in normal and neoplastic pituitary tissue. Endocr Rev *12*, 337-355.
Fu, Q., and Vankelecom, H. (2012). Regenerative capacity of the adult pituitary: multiple mechanisms of lactotrope restoration after transgenic ablation. Stem Cells Dev *21*, 3245-3257.
Gage, P.J., Brinkmeier, M.L., Scarlett, L.M., Knapp, L.T., Camper, S.A., and Mahon, K.A. (1996). The Ames dwarf gene, df, is required early in pituitary ontogeny for the extinction of Rpx transcription and initiation of lineage-specific cell proliferation. Mol Endocrinol *10*, 1570-1581.
Gaylinn, B.D. (2002). Growth hormone releasing hormone receptor. Receptors Channels *8*, 155-162.
Gill, B.M., Barbosa, J.A., Dinh, T.Q., Garrod, S., and O'Connor, D.T. (1991). Chromogranin B: isolation from pheochromocytoma, N-terminal sequence, tissue distribution and secretory vesicle processing. Regul Pept *33*, 223-235.
Gleiberman, A.S., Michurina, T., Encinas, J.M., Roig, J.L., Krasnov, P., Balordi, F., Fishell, G., Rosenfeld, M.G., and Enikolopov, G. (2008). Genetic approaches identify adult pituitary stem cells. Proc Natl Acad Sci U S A *105*, 6332-6337.
Guerreiro, R.J., Gustafson, D.R., and Hardy, J. (2012). The genetic architecture of Alzheimer's disease: beyond APP, PSENs and APOE. Neurobiol Aging *33*, 437-456.
Hammer, R.E., Brinster, R.L., Rosenfeld, M.G., Evans, R.M., and Mayo, K.E. (1985). Expression of human growth hormone-releasing factor in transgenic mice results in increased somatic growth. Nature *315*, 413-416.
Han, X., Wang, R., Zhou, Y., Fei, L., Sun, H., Lai, S., Saadatpour, A., Zhou, Z., Chen, H., Ye, F.*, et al.* (2018). Mapping the Mouse Cell Atlas by Microwell-Seq. Cell *173*, 1307.
Ho, Y., Elefant, F., Cooke, N., and Liebhaber, S. (2002). A defined locus control region determinant links chromatin domain acetylation with long-range gene activation. Mol Cell *9*, 291-302.
Ho, Y., Shewchuk, B.M., Liebhaber, S.A., and Cooke, N.E. (2013). Distinct chromatin configurations regulate the initiation and the maintenance of hGH gene expression. Mol Cell Biol *33*, 1723-1734.

Ho, Y., Tadevosyan, A., Liebhaber, S.A., and Cooke, N.E. (2008). The juxtaposition of a promoter with a locus control region transcriptional domain activates gene expression. EMBO Rep *9*, 891-898.
Hu, P., Fabyanic, E., Kwon, D.Y., Tang, S., Zhou, Z., and Wu, H. Dissecting Cell-Type Composition and Activity-Dependent Transcriptional State in Mammalian Brains by Massively Parallel Single-Nucleus RNA-Seq. Molecular Cell *68*, 1006-1015.e1007.
Hu, P., Fabyanic, E., Kwon, D.Y., Tang, S., Zhou, Z., and Wu, H. (2017). Dissecting Cell-Type Composition and Activity-Dependent Transcriptional State in Mammalian Brains by Massively Parallel Single-Nucleus RNA-Seq. Mol Cell *68*, 1006-1015 e1007.
Ingraham, H.A., Lala, D.S., Ikeda, Y., Luo, X., Shen, W.H., Nachtigal, M.W., Abbud, R., Nilson, J.H., and Parker, K.L. (1994). The nuclear receptor steroidogenic factor 1 acts at multiple levels of the reproductive axis. Genes Dev *8*, 2302-2312.
Inoue, K., Mogi, C., Ogawa, S., Tomida, M., and Miyai, S. (2002). Are folliculo-stellate cells in the anterior pituitary gland supportive cells or organ-specific stem cells? Arch Physiol Biochem *110*, 50-53.
Janknecht, R. (2010). Multi-talented DEAD-box proteins and potential tumor promoters: p68 RNA helicase (DDX5) and its paralog, p72 RNA helicase (DDX17). Am J Transl Res *2*, 223-234.
Kelberman, D., Rizzoti, K., Lovell-Badge, R., Robinson, I.C., and Dattani, M.T. (2009). Genetic regulation of pituitary gland development in human and mouse. Endocr Rev *30*, 790-829.
Lamberts, S.W., and Macleod, R.M. (1990). Regulation of prolactin secretion at the level of the lactotroph. Physiol Rev *70*, 279-318.
Lamolet, B., Pulichino, A.M., Lamonerie, T., Gauthier, Y., Brue, T., Enjalbert, A., and Drouin, J. (2001). A pituitary cell-restricted T box factor, Tpit, activates POMC transcription in cooperation with Pitx homeoproteins. Cell *104*, 849-859.
Le Tissier, P.R., Hodson, D.J., Lafont, C., Fontanaud, P., Schaeffer, M., and Mollard, P. (2012). Anterior pituitary cell networks. Front Neuroendocrinol *33*, 252-266.
Le Tissier, P.R., Hodson, D.J., Martin, A.O., Romano, N., and Mollard, P. (2015). Plasticity of the prolactin (PRL) axis: mechanisms underlying regulation of output in female mice. Adv Exp Med Biol *846*, 139-162.
Li, S., Crenshaw, E.B., 3rd, Rawson, E.J., Simmons, D.M., Swanson, L.W., and Rosenfeld, M.G. (1990). Dwarf locus mutants lacking three pituitary cell types result from mutations in the POU-domain gene pit-1. Nature *347*, 528-533.
Lin, S.C., Lin, C.R., Gukovsky, I., Lusis, A.J., Sawchenko, P.E., and Rosenfeld, M.G. (1993). Molecular basis of the little mouse phenotype and implications for cell type-specific growth. Nature *364*, 208-213.
Liu, N.A., Liu, Q., Wawrowsky, K., Yang, Z., Lin, S., and Melmed, S. (2006). Prolactin receptor signaling mediates the osmotic response of embryonic zebrafish lactotrophs. Mol Endocrinol *20*, 871-880.
Luque, R.M., Amargo, G., Ishii, S., Lobe, C., Franks, R., Kiyokawa, H., and Kineman, R.D. (2007). Reporter expression, induced by a growth hormone promoter-driven Cre recombinase (rGHp-Cre) transgene, questions the developmental relationship between somatotropes and lactotropes in the adult mouse pituitary gland. Endocrinology *148*, 1946-1953.

Macosko, E.Z., Basu, A., Satija, R., Nemesh, J., Shekhar, K., Goldman, M., Tirosh, I., Bialas, A.R., Kamitaki, N., Martersteck, E.M., *et al.* (2015). Highly Parallel Genome-wide Expression Profiling of Individual Cells Using Nanoliter Droplets. Cell *161*, 1202-1214.
Mayo, K.E., Hammer, R.E., Swanson, L.W., Brinster, R.L., Rosenfeld, M.G., and Evans, R.M. (1988). Dramatic pituitary hyperplasia in transgenic mice expressing a human growth hormone-releasing factor gene. Mol Endocrinol *2*, 606-612.
Mayo, K.E., Miller, T., DeAlmeida, V., Godfrey, P., Zheng, J., and Cunha, S.R. (2000). Regulation of the pituitary somatotroph cell by GHRH and its receptor. Recent Prog Horm Res *55*, 237-266; discussion 266-237.
Mayran, A., Khetchoumian, K., Hariri, F., Pastinen, T., Gauthier, Y., Balsalobre, A., and Drouin, J. (2018). Pioneer factor Pax7 deploys a stable enhancer repertoire for specification of cell fate. Nat Genet *50*, 259-269.
Michael, S.D., Kaplan, S.B., and Macmillan, B.T. (1980). Peripheral plasma concentrations of LH, FSH, prolactin and GH from birth to puberty in male and female mice. J Reprod Fertil *59*, 217-222.
Nakajima, T., Yamaguchi, H., and Takahashi, K. (1980). S100 protein in folliculostellate cells of the rat pituitary anterior lobe. Brain Res *191*, 523-531.
Nakane, P.K. (1970). Classifications of anterior pituitary cell types with immunoenzyme histochemistry. J Histochem Cytochem *18*, 9-20.
Nishida, Y., Yoshioka, M., and St-Amand, J. (2005). Sexually dimorphic gene expression in the hypothalamus, pituitary gland, and cortex. Genomics *85*, 679-687.
Nunez, L., Villalobos, C., Senovilla, L., and Garcia-Sancho, J. (2003). Multifunctional cells of mouse anterior pituitary reveal a striking sexual dimorphism. J Physiol *549*, 835-843.
Ohta, K., Nobukuni, Y., Mitsubuchi, H., Fujimoto, S., Matsuo, N., Inagaki, H., Endo, F., and Matsuda, I. (1992). Mutations in the Pit-1 gene in children with combined pituitary hormone deficiency. Biochem Biophys Res Commun *189*, 851-855.
Peel, M.T., Ho, Y., and Liebhaber, S.A. (2018). Transcriptome analyses of female somatotropes and lactotropes reveal novel regulators of cell identity in the pituitary. Endocrinology.
Perez Millan, M.I., Brinkmeier, M.L., Mortensen, A.H., and Camper, S.A. (2016). PROP1 triggers epithelial-mesenchymal transition-like process in pituitary stem cells. Elife *5*.
Philips, A., Maira, M., Mullick, A., Chamberland, M., Lesage, S., Hugo, P., and Drouin, J. (1997). Antagonism between Nur77 and glucocorticoid receptor for control of transcription. Mol Cell Biol *17*, 5952-5959.
Radovick, S., Nations, M., Du, Y., Berg, L.A., Weintraub, B.D., and Wondisford, F.E. (1992). A mutation in the POU-homeodomain of Pit-1 responsible for combined pituitary hormone deficiency. Science *257*, 1115-1118.
Ragoczy, T., Bender, M.A., Telling, A., Byron, R., and Groudine, M. (2006). The locus control region is required for association of the murine beta-globin locus with engaged transcription factories during erythroid maturation. Genes Dev *20*, 1447-1457.

Scholzen, T., and Gerdes, J. (2000). The Ki‐67 protein: From the known and the unknown. Journal of Cellular Physiology *182*, 311-322.
Seuntjens, E., Hauspie, A., Roudbaraki, M., Vankelecom, H., and Denef, C. (2002a). Combined expression of different hormone genes in single cells of normal rat and mouse pituitary. Arch Physiol Biochem *110*, 12-15.
Seuntjens, E., Hauspie, A., Vankelecom, H., and Denef, C. (2002b). Ontogeny of plurihormonal cells in the anterior pituitary of the mouse, as studied by means of hormone mRNA detection in single cells. J Neuroendocrinol *14*, 611-619.
Shekhar, K., Lapan, S.W., Whitney, I.E., Tran, N.M., Macosko, E.Z., Kowalczyk, M., Adiconis, X., Levin, J.Z., Nemesh, J., Goldman, M.*, et al.* (2016). Comprehensive Classification of Retinal Bipolar Neurons by Single-Cell Transcriptomics. Cell *166*, 1308-1323 e1330.
Tanay, A., and Regev, A. (2017). Scaling single-cell genomics from phenomenology to mechanism. Nature *541*, 331-338.
Theogaraj, E., John, C.D., Christian, H.C., Morris, J.F., Smith, S.F., and Buckingham, J.C. (2005). Perinatal glucocorticoid treatment produces molecular, functional, and morphological changes in the anterior pituitary gland of the adult male rat. Endocrinology *146*, 4804-4813.
Traverso, V., Christian, H.C., Morris, J.F., and Buckingham, J.C. (1999). Lipocortin 1 (annexin 1): a candidate paracrine agent localized in pituitary folliculo-stellate cells. Endocrinology *140*, 4311-4319.
Tyssowski, K.M., DeStefino, N.R., Cho, J.H., Dunn, C.J., Poston, R.G., Carty, C.E., Jones, R.D., Chang, S.M., Romeo, P., Wurzelmann, M.K.*, et al.* (2018). Different Neuronal Activity Patterns Induce Different Gene Expression Programs. Neuron *98*, 530-546 e511.
Vazquez-Borrego, M.C., Gahete, M.D., Martinez-Fuentes, A.J., Fuentes-Fayos, A.C., Castano, J.P., Kineman, R.D., and Luque, R.M. (2018). Multiple signaling pathways convey central and peripheral signals to regulate pituitary function: Lessons from human and non-human primate models. Mol Cell Endocrinol *463*, 4-22.
Vidal, S., Horvath, E., Kovacs, K., Lloyd, R.V., and Smyth, H.S. (2001). Reversible transdifferentiation: interconversion of somatotrophs and lactotrophs in pituitary hyperplasia. Mod Pathol *14*, 20-28.
Villalobos, C., Nunez, L., and Garcia-Sancho, J. (2004a). Anterior pituitary thyrotropes are multifunctional cells. Am J Physiol Endocrinol Metab *287*, E1166-1170.
Villalobos, C., Nunez, L., and Garcia-Sancho, J. (2004b). Phenotypic characterization of multi-functional somatotropes, mammotropes and gonadotropes of the mouse anterior pituitary. Pflugers Arch *449*, 257-264.
Willems, C., Fu, Q., Roose, H., Mertens, F., Cox, B., Chen, J., and Vankelecom, H. (2016). Regeneration in the Pituitary After Cell-Ablation Injury: Time-Related Aspects and Molecular Analysis. Endocrinology *157*, 705-721.
Zheng, G.X., Terry, J.M., Belgrader, P., Ryvkin, P., Bent, Z.W., Wilson, R., Ziraldo, S.B., Wheeler, T.D., McDermott, G.P., Zhu, J.*, et al.* (2017). Massively parallel digital transcriptional profiling of single cells. Nat Commun *8*, 14049.

Zhu, X., Gleiberman, A.S., and Rosenfeld, M.G. (2007). Molecular physiology of pituitary development: signaling and transcriptional networks. Physiol Rev *87*, 933-963.
Zhu, X., Tollkuhn, J., Taylor, H., and Rosenfeld, M.G. (2015). Notch-Dependent Pituitary SOX2(+) Stem Cells Exhibit a Timed Functional Extinction in Regulation of the Postnatal Gland. Stem Cell Reports *5*, 1196-1209.

Figure Legends.

Figure 1. Single cell transcriptome analysis of the mouse pituitary

A. Clustering of adult pituitary cells based on principal component analysis of single cell transcriptomes. The spectral tSNE plot reflects the clustering analysis of individual adult pituitary cell transcriptomes (n = 6,995). The data represent the summation of 4 independent studies of pituitaries isolated from 7-8 week old, sexually naive male and female mice. Each color-coded cluster was assigned an 'identity' based on the expression of sets of informative markers (as in **C** below; see text for details).

B. Expression of a subset of the marker genes used to assign cell cluster identities. The violin plots summarize mRNA expression corresponding to each indicated gene. The provisional identification of each cluster is noted at the bottom of each corresponding lane. Clusters corresponding to hormone expressing cells and those corresponding to the interstitial folliculostellate (FS) cells are bracketed above the corresponding lanes.

C. Distributions of mRNAs encoding the pituitary transcription factor *Pou1f1*, the signal receptor Ghrhr, and six pituitary hormones. These distributions are superimposed on the cell cluster diagram (**A**). Each feature map is labeled according to its respective mRNA. The heat map legend is displayed to the right.

Figure 2. *Gh* and *Prl* mRNAs are co-expressed in the majority of cells in the mouse pituitary.

A. Single cell RNA fluorescent *in situ* hybridization (scFISH) of adult mouse pituitary cells reveals a concordance of *Gh* with *Prl* expression.

Left panel: *Prl* mRNA detection. *Prl* mRNAs were detected by FISH using an array of Alex 488-conjugated anti-sense oligos. The white arrows indicate three cells with robust *Prl* mRNA accumulation and the orange arrows indicate an additional four cells with lower levels of *Prl* mRNA accumulation.

Middle panel: ***Gh* mRNA detection**. *GH* mRNA was detected by FISH using an array of Cy3-conjugated anti-sense oligos. The white arrows indicate cells with robust *Gh* mRNA expression and the orange arrows indicate an additional four cells expressing lower levels of *Gh* mRNA.

Right panel: DAPI (nuclear) stain. Field is the same as in **a** and **b.** Bars = 5 μm.

B. Quantification of cells co-expressing *Gh* and *Prl* mRNAs.

Left graph: analysis of male pituitary cells. Cells from 7-8 week old, sexually naïve male mice (n = 986) were analyzed by scRNA FISH (as in **A**.) for *Gh* and/or *Prl* mRNA expression. The histogram represents the percent of the total cell population positive for both *Gh* and *Prl* mRNA (Gh^+Prl^+ ; 61.6%), positive for *Gh* but not *Prl* mRNA (Gh^+Prl^-; 6.3%) and positive for Prl but not Gh mRNA (Gh^-Prl^+; 0%).

Right graph: analysis of female pituitary cells. Cells from 7-8 week old, sexually naïve adult female mice (n = 423) were analyzed by RNA FISH. The histogram displays the representation of dual positive cells (Gh^+Prl^+; 65.5%), cells positive for *Gh* but not *Prl* mRNA (Gh^+Prl^-; 6.9%) and those positive for *Prl* but not *Gh* mRNA (Gh^-Prl^+; 16.5).

Figure 3. Combined single cell IF protein detection and RNA FISH analysis (scIF/RNA FISH) confirms co-expression of *Gh* and *Prl* genes.

A. Detection of Prl and Gh proteins by immunofluorescent (IF) analyses paired with detection of *Gh* mRNA by scFISH. Examples of various combinations of protein and RNA expression are shown in this field. The white arrow identifies a cell that is strongly positive for Prl protein and negative for Gh protein and contains trace levels of *Gh* mRNA. The red arrow indicates a cell that is strongly positive for *Gh* mRNA and protein and negative for Prl protein. The yellow arrow indicates a cell that is positive for both Prl and Gh proteins (Gh > Prl). The cells strongly positive for Gh (yellow and red arrows) contain robust levels of *Gh* mRNA and cells with less pronounced IF signals for Gh protein (orange arrows) have correspondingly weaker signals for *Gh* mRNA. Scale bar=5 μm.

B. Detection of PRL and GH proteins by IF analysis paired with *Prl* mRNA scRNA-FISH. Details as in **A**., above. The yellow arrow indicates a cell that is positive for both Prl and GH proteins and contains robust levels of *Prl* mRNA. The red arrows point to three GH+ cells that are negative for Prl protein, but contain low levels of *Prl* mRNA. Scale bar; 5 μm.

Figure 4. *Tshb* mRNA maps to the multi-hormone cluster (Mult) and is predominantly co-expressed along with *Gh* and *Prl* mRNAs.

A. 3D scatter plot of *Tshb, Gh,* and *Prl* mRNAs. This analysis of Drop-seq data reveals that majority of the *Tshb* expressing cells co-express *Gh* and/or *Prl* mRNA. The levels of *Tshb*, *Gh*, and *Prl* mRNAs are represented on each of three labeled axes. The 3D plot

identifies subsets of cells uniquely expressing either *Prl* (predominantly in female samples) or uniquely expressing *Gh* mRNAs (predominantly in male samples). The Drop-seq data are remarkable in revealing that only 8.7% of the total number of *Tshb*+ cell expressing in the analysis (n =436) express *Tshb* mRNA in the absence of *Gh* or *Prl* mRNAs. (Corresponding sets of 2D scatter plots representing these data are shown in Suppl **Fig. S3**)

B. *Tshβ* and *Gh* co-expression as revealed by combined scIF/FISH. Detection of Tshβ protein (panel a; green) and Gh protein (panel b; red) was performed by IF and *Gh* RNA detection was established by scFISH (panel c; gray). This single field analysis is representative of pituitary cells from a male mouse. The white arrow indicates a cell positive for Tshβ protein that co-expresses Gh protein (middle panel) and *Gh* mRNA (right panel). For comparison, the orange arrow indicates a cell expressing Gh protein and *Gh* mRNA in the absence of Tshβ protein, and the red arrow indicates a cell that is expressing of Gh protein and *Gh* mRNA along with a low level of Tshβ protein. Nuclei were stained with DAPI (blue). Scale bar; 5 μm.

C. Summary of the analysis of cells expressing Tshβ and/or Gh. The cells were isolated from a male mouse pituitary (n = 141). All cells positive for Tshβ protein on IF expressed *Gh* mRNA by FISH either at robust levels (Gh++; 81.6%) (ex: red arrow) or low levels (Gh+; 18.4%) (ex; white arrow).

Figure 5. Clustering analysis of scRNA-seq data reveals sexual dimorphism in pituitary cell composition.

A. Spectral tSNE plot of cells isolated from male (n= 3,689; left panel) and female (n = 3,536; right panel) pituitaries in the (as in **Figs. 2, 3).**

B. Sexual dimorphism of the pituitary cell composition. The histogram summarizes the relative distributions of cells in the male and female pituitary in each defined cluster, (derived from A.). These data reveal that the male pituitary has a relative enrichment for somatotropes with a reciprocal enrichment for lactotropes in the female pituitary. Analysis of the *Pou1f1*-negative clusters reveals a significant enrichment of gonadotropes in the males reflecting a higher concentration of *Fshb* mRNA.

Figure 6. Single cell transcriptome analysis of the pituitary cells of lactating mice

A. Clustering of adult pituitary cells based on principal component analysis of single cell transcriptomes. The spectral tSNE plot reflects the clustering analysis of individual adult pituitary cell transcriptomes (n = 10,860). The data represent the summation of pituitaries isolated from four 13 week old female mice (three lactating and one non-lactating). Each color-coded cluster was assigned an 'identity' based on the expression of sets of informative markers (see text for details).

B. The pituitary cell composition in lactating females. The histogram shows the representation in cell corresponding to each indicated cluster in a control and each of two experiments (lac2 contains two lactating mice).

C. Differential gene expression analysis of the lactotropes from lactating and sexual naïve mice. The analysis was performed from 1,052 lactotropes from control and 3,381 lactotropes from lactating mice, respectively. Cells originating from the lactating females are in orange and those from the age/sex matched control are in green.

D. Enhanceent of *Prl* expression in lactotropes of lactating female mice. The expression of Prl in each cell originating from lactating and control mice is displayed (heat map shown to the right); the distribution of the cells from the control and lactating mice is as in A.

E. Induction of *Chgb* expression in lactotropes during lactation. The expression of Chgb mRNA was analyzed from the lactotropes of lactating and control mice, respectively. The distribution of the cells from the control and lactating mice is as in A.

D. Differential gene expression analysis of cells in the multi-hormone, somatotrope , and lactotrope clusters during lactation.

Left panel. Multi-hormone cluster. The analysis compared the levels of expression of genes in the multihormone cluster in lactating females (n = 786) with an age matched female control (n = 379). Each dot represents mRNA expression from a specific gene. The volcano plot shows the Log_2 fold change [log_2FC(lactation/control)] in this value between the two groups on the X-axis and the Log_{10} p-value of the binary comparison for each gene on the Y-axis. Genes of particular interest (*Prl*, *Gh*, *Lhb*, and *Nr4a2*) are indicated as labeled red dots (details in text).

Middle panel. Somatotrope cluster. The analysis was performed using 1591 somatotropes from lactating mice compared with 714 somatotropes from an age matched female control. The volcano plot is organized as in left panel and highlights genes of particular interest (*Prl* and *Gh)* (details in text).

Right panel. Lactotrope cluster. The analysis was performed using 3376 lactotropes from lactating mice compared with 1052 lactotropes from an age matched

female control. The volcano plot is organized as in left panel and highlights genes of particular interest (*Prl* and *Chgb*) (details in text)

Figure 7. Single cell transcriptome analysis of the pituitary cells of mice overexpressing an *hGhrh* transgene

A. Clustering of adult pituitary cells based on principal component analysis of single cell transcriptomes in *hGhrh* transgenic mice. The spectral tSNE plot reflects the clustering analysis of individual adult pituitary cell transcriptomes (n =2,842) from two 8 week old female *hGhrh* transgenic mice. Each color-coded cluster was assigned an 'identity' based on the expression of sets of informative markers (see text for details). The Pomc+ cluster includes both melanotropes and corticotropes.

B. The pituitary cell composition in WT and *hGhrh* transgenic mice. The histogram shows the cell composition in the transgenic and 8 week old female CD1 (non-transgenic control; WT) mouse pituitary, respectively.

C. Differential gene expression analysis of the Pou1f1^{+} lineages in *hGhrh* transgenic mice

Left panel. The comparison of the transcriptomes of lactotropes from WT and *hGhrh* transgenic mice. The volcano plot (configured as in **Fig. 8**) shows the genes in which the expression was significantly altered during lactation. The positions of Prl, *Gh*, and *POMC* are labeled in red (details see text).

Middle panel. The comparison of the transcriptomes of somatotropes from WT and *hGhrh* transgenic mice. The positions of Prl, *Gh*, and *POMC* are labeled in red (details see text).

Right panel. The comparison of the transcriptomes of multi-hormone cluster from WT and *hGhrh* transgenic mice. The positions of Prl, *Gh*, *Lhb* and *POMC* are labeled in red (details see text).

Supplemental Figure Legends

Figure S1. Standard model of anterior pituitary development and lineage specification

This diagram summarizes the current model of pituitary lineage differentiation. The development of the mouse anterior pituitary from the oral ectoderm is driven by a complex array of signaling pathways and transcription factors, a subset of which are indicated. The adult pituitary is characterized by the presence of six terminally differentiated cell types, each defined by the expression of its corresponding hormone (Prl, prolactin; Gh, growth hormone; Tshb; β subunit of thyroid stimulating hormone; Lhβ and Fshβ, the β subunits of the luteinizing and follicle stimulating hormones; POMC, proopiomelanocortin prohormone; ACTH, adrenocorticotropic hormone; α-MSH, melanocyte stimulating hormone). Differentiation of three lineages (lactotropes, somatotropes and thyrotropes) is specifically driven by, and dependent on, the POU-homeo domain transcription factor, Pou1f1. The remaining three lineages (corticotropes, melanotropes, and gonadotropes) are considered to be Pou1f1-independent.

Figure S2. Background correction, stress-induced effect regression, and clustering parameter choices for single cell RNA-seq data

A. Comparison of PCA analysis results between with and without stress-induced effect maintaining the same clustering parameter settings. Before regressing out stress-induced genes, PC4 (left panel), which accounts for 3.45% of total variation, is

dominated by the stress-related genes, including *Fos*, *Junb*, *Egr1* and *Btg2* (highlighted by red). Right panel shows the top leading genes of first top 4 PCs.

B. Robustness of tSNE clustering to variation of number of PCs. t-SNE plots show the effect of varying PC numbers as shown in the title above the plot.

C. Robustness of tSNE clustering to variation in resolution parameters. Left 3 plots respond to resolution 0.6, 1 and 2, respectively. The right most panel showing the cluster merge results after 10% OOBE of resolution 1 clustering results, which is consistence with the clustering results of resolution 0.6.

D. **The tSNE plot colored according to sex.**

E. **Bar plot of cluster distribution across 4 sample batches.**

Figure S3. Dendrogram showing relatedness of the 4 major Pou1f1+ lineages

The average expression of marker genes was centered and scaled by each gene. The hclust function in the R was used to generate the cluster dendrogram with the "ward.D" method. The data reveal the concordance of the Lac1 and Lac2 in the transcriptomes despite the absence of *Prl* in the Lac2 cluster.

Figure S4. 2D scatter plots of hormone expression in cells encompassed in the major Pou1f1 clusters (somatotrope, lactotrope (Lac1 and Lac2), and multi-hormone) of male (blue) and female (red) pituitaries.

A. Co-expression of *Gh*, *Prl*, and *Tshb*. The 2D scatter graphs plot *Gh vs Prl, Tshb vs Prl,* and *Gh vs Tshb*. Of note: *(1)* the majority of *Tshb* mRNA is localized to multi-hormone cluster, the remainder in somatotrope cluster with very few *Tshb*-positive cells

in lactotrope clusters (Lac 1 and Lac2); *(2)* 91.3% *Tshb*-expressing cells co-express *Gh* and/or *Prl* although many *Gh*-expressing and *Prl*-expressing cells lack *Tshb* expression.

B. Co-expression of *POMC* with *Gh*, *Prl*, and *Tshb* mRNAs. 2D scatter plots relate the co-expression of mRNAs encoding *POMC* with those encoding *Gh*, *Prl*, and *Tshb*. Of note: *(1)* the great majority of cells expressing *Gh, Prl,* or *Tshb* co-express *POMC*, *(2) Gh* mRNA is co-expressed in the vast majority of $POMC^+$ cells in multi-hormone cluster, *(3)* the great majority of the *Tshb*-expressing cells co-express *POMC*.

C. Co-expression of *Lhb* mRNA with mRNAs encoding Gh, Prl, and Tshb. 2D scatter plots reveal: *(1) Lhb* mRNA expression is uniformly accompanied with co-expression of both *Gh* and *Prl* mRNAs, *(2)* expression of *Tshb* and *Lhb* mRNAs are mutually exclusive in lactotropes, predominantly mutually exclusive in somatotropes, while in multi-hormone cluster there is substantial coordinate co-expression of the two genes.

Figure S5. *POMC* mRNA is co-expressed with *Gh* and/or *Prl* mRNAs in the majority of mouse pituitary cells.

A. *Gh* and *POMC* mRNAs are co-expressed in majority of the pituitary cells.

Left and Right panels: *Gh* mRNAs were detected by FISH using an array of Cy3-conjugated anti-sense oligonucleotide probes (Left panel). *POMC* mRNA was detected by FISH using an array of Cy5-conjugated anti-sense oligonucleotide probes (Right panel). The white arrow indicates a cell with robust co-expression of *Gh* and *Pomc* mRNAs and the orange arrows indicate an additional three cells with weaker signals for the two co-expressed mRNAs. The nuclei were stained with DAPI (blue).

Histogram summarizes the number of POMC+ cells that were positive for both *Gh* and *POMC* mRNA (*Gh*$^{+}$*Prl*$^{+}$; 65%) or positive for *POMC* but not *Gh* mRNA (*POMC*$^{+}$/Gh*l*$^{-}$; 15%).

B. *Prl* and *POMC* mRNAs are co-expressed in majority of the pituitary cells.

Left and Right panel: *Prl* mRNAs were detected using an array of Alexa fluro 488-conjugated anti-sense oligonucleotide probes. *POMC* mRNA was detected as described in **A**. The two white arrows indicate two cells with robust co-expression of *Prl* and *Pomc* mRNAs and the orange arrows indicate a additional two cells with weaker signals for the two co-expressed mRNAs. The nuclei were stained with DAPI (blue).

Histogram summarizes the number of dual positive cells (*POMC*$^{+}$*Prl*$^{+}$; 74%), cells positive for *POMC* but not *Prl* mRNA (*POMC*$^{+}$/*Prl*$^{-}$; 6%).

Figure S6. Single cell transcriptome analysis of the mouse pituitary from 13 week old female mice

The Drop-seq was performed in one 13 week old, sex naïve female mouse and three 13 week old lactating mice (two weeks into lactation in two independent replicates**).** Each replicate is color-coded. The lactotrope cluster is outlined with dashed line. The lactotropes from the control mouse and the lactating mice are labeled.

Table S1. List of marker genes in each cluster.

Fig. 1

A

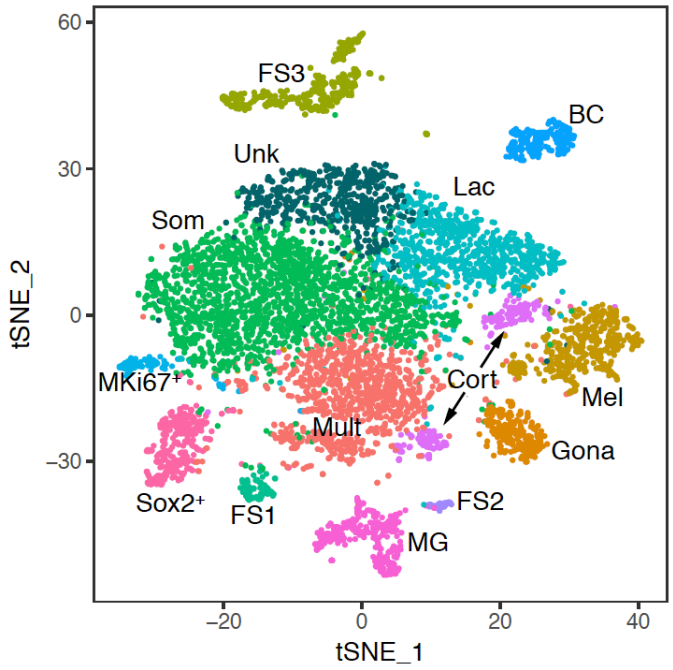

Som - Somatotrope
Lac- Lactotrope
Unk- Lactotrope related cluster (Unknown)
Mult – Multi-hormone producing cells
Mki67+ - Proliferating Pou1f1+ cells
Gona - Gonadotrope
Cort – Corticotrope
Mel – Melanotrope
Sox2+ - Adult Stem cell
FS 1-3 – Folliculostellate cell 1-3
MG - Microglia
BC – Blood cell

B

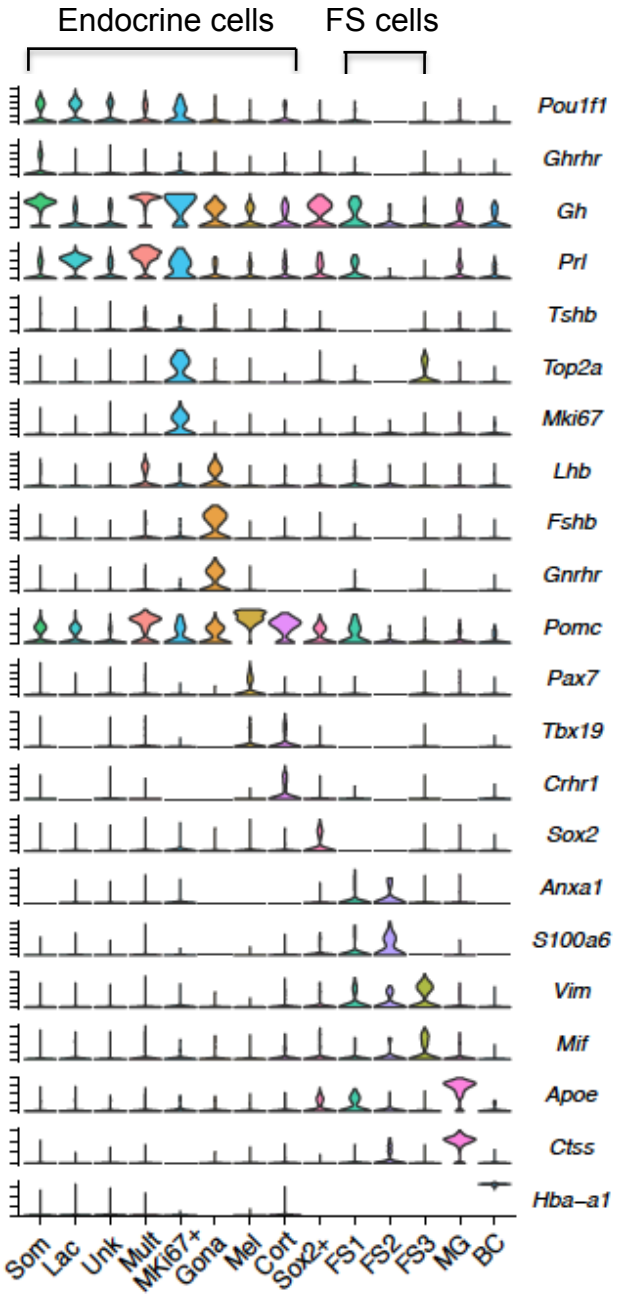

Fig.1C

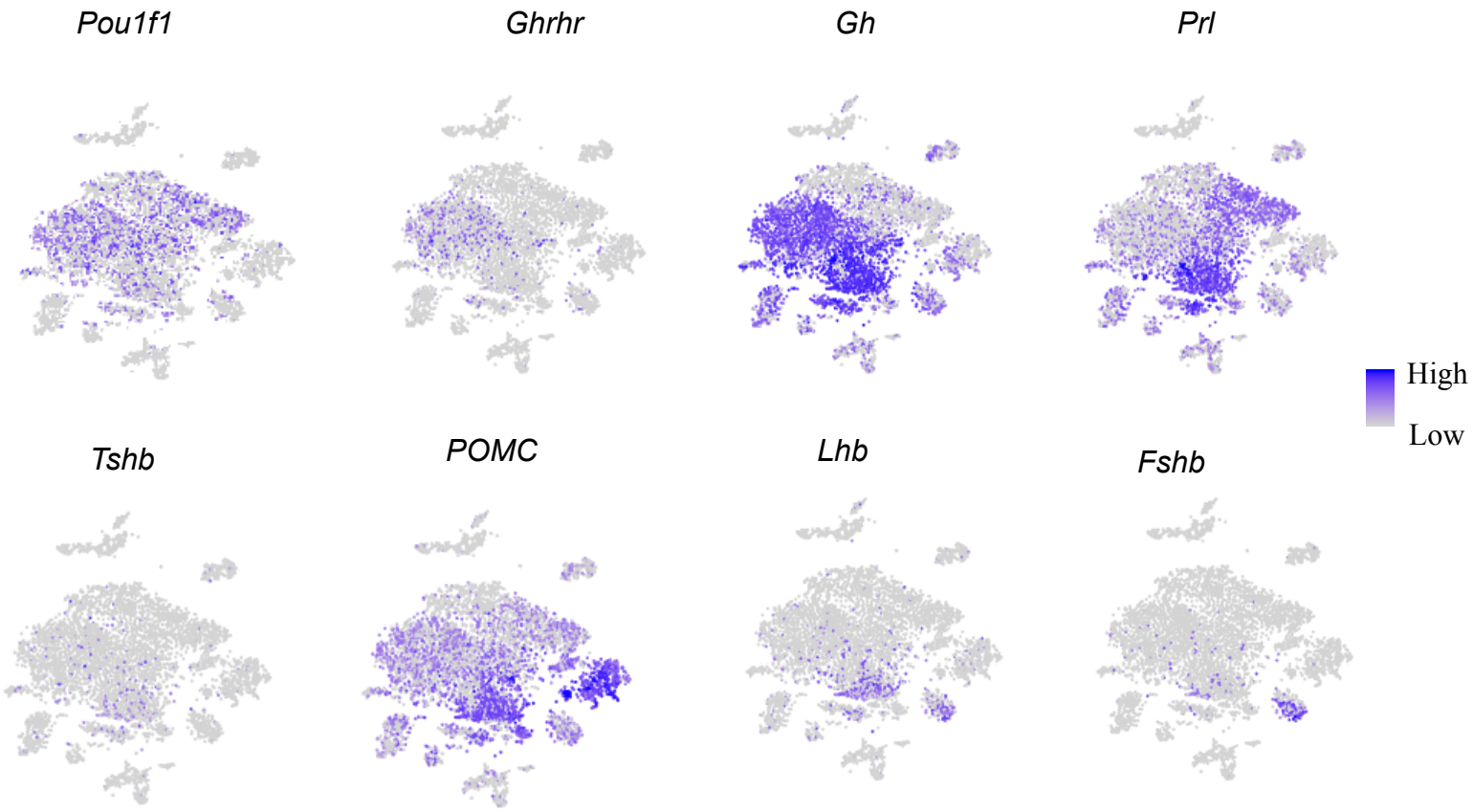

Fig. 2

A

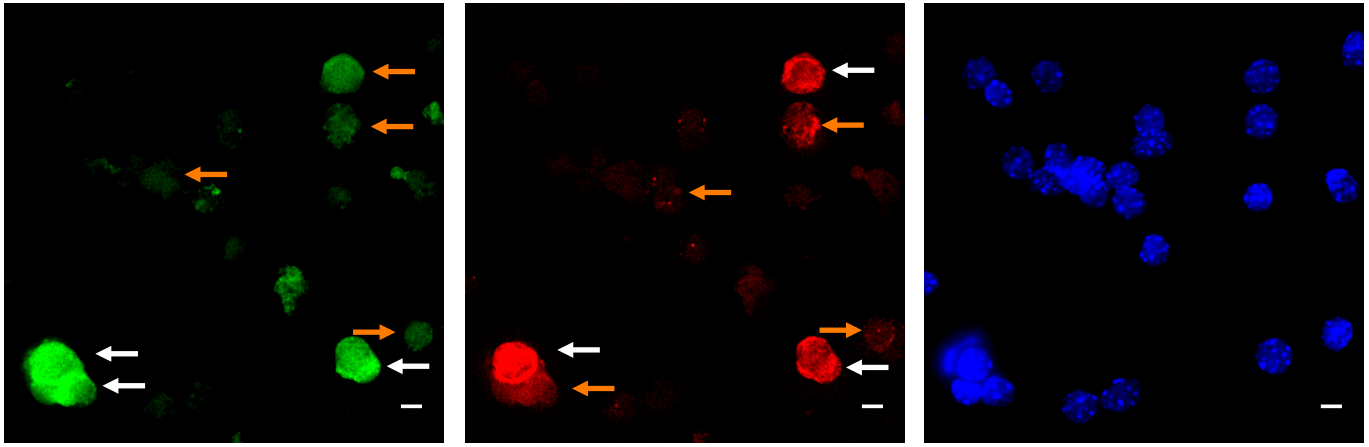

Prl RNA FISH (Green)

Gh RNA FISH (Red)

DAPI (Blue)

B

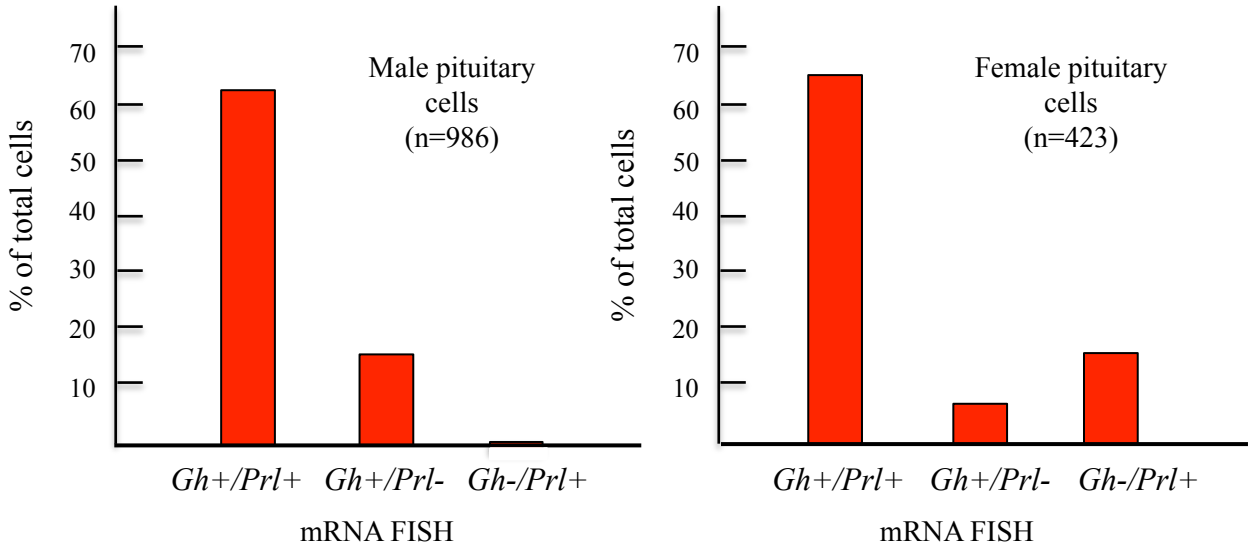

Fig. 3

A

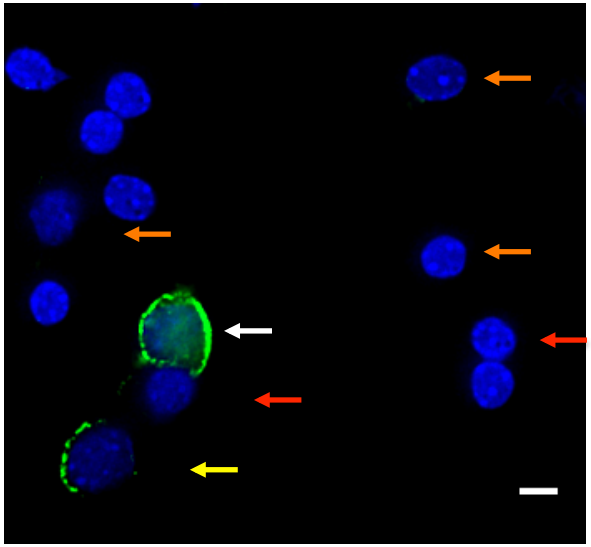

Prl IF (Green)

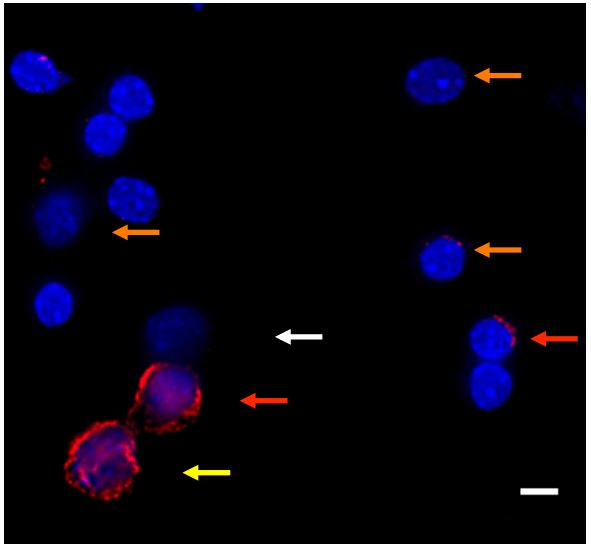

Gh IF (Red)

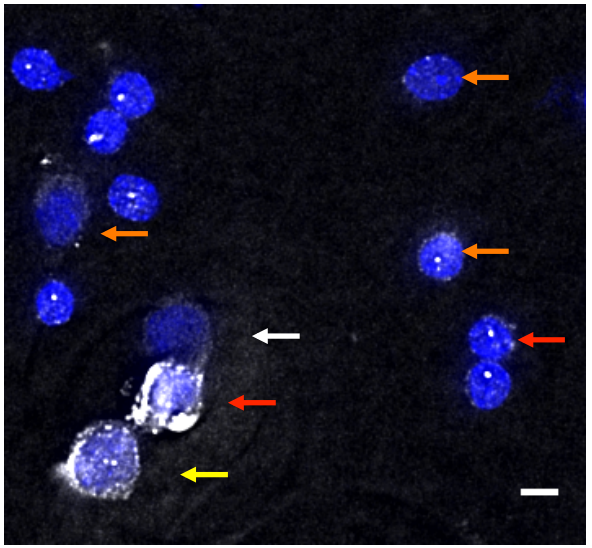

Gh RNA FISH (Gray)

B

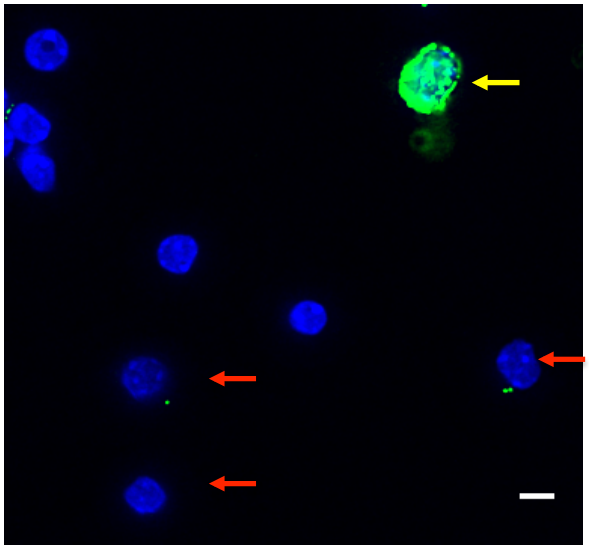

Prl IF (Green)

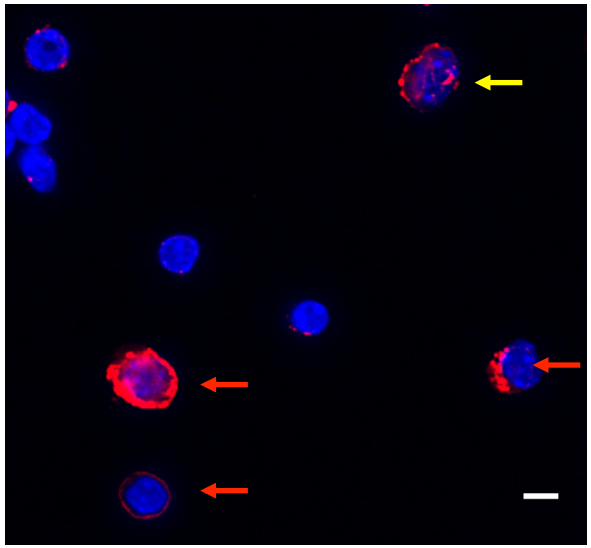

Gh IF (Red)

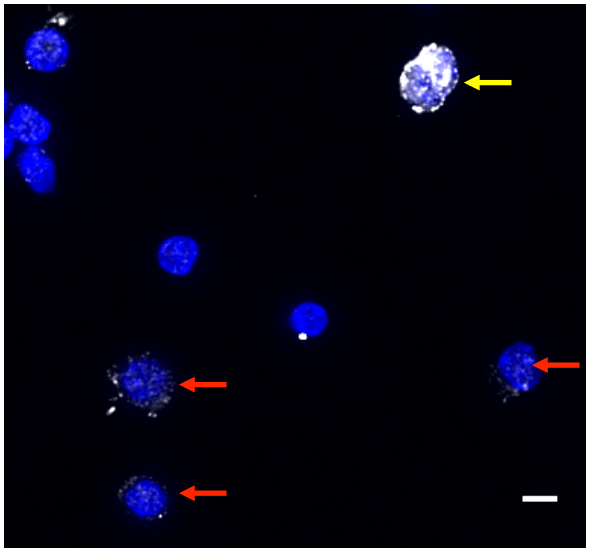

Prl RNA FISH (Gray)

Fig. 4

A

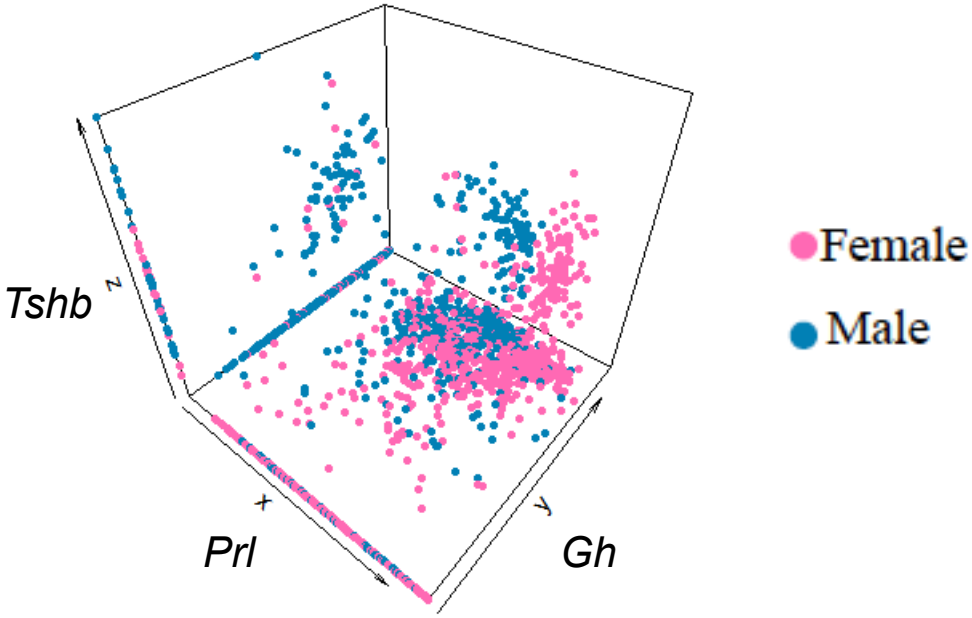

B

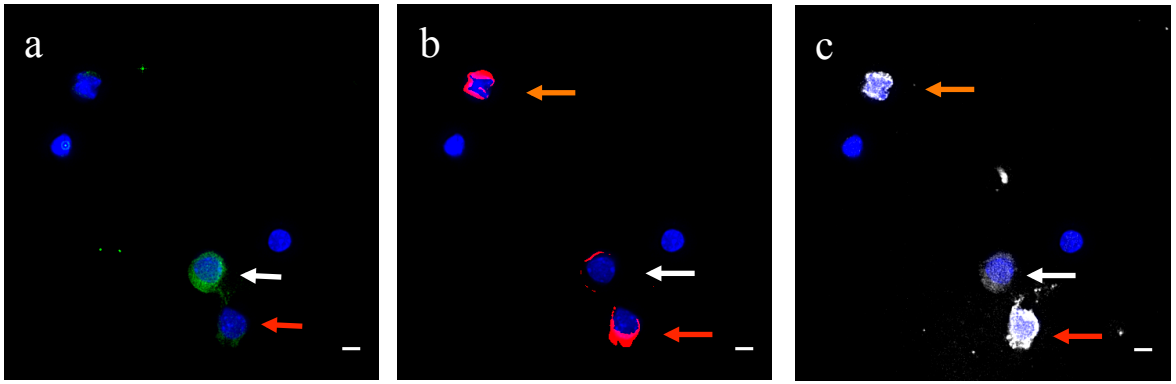

Tshb (green) Gh (red) *Gh* RNA (grey)

C

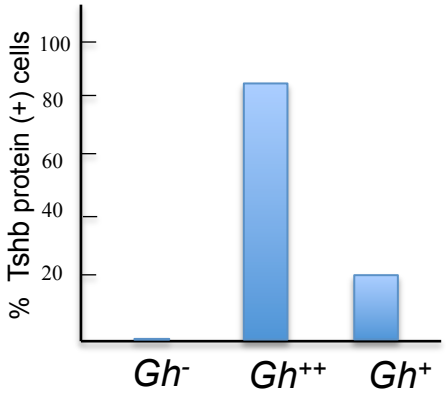

Fig.5

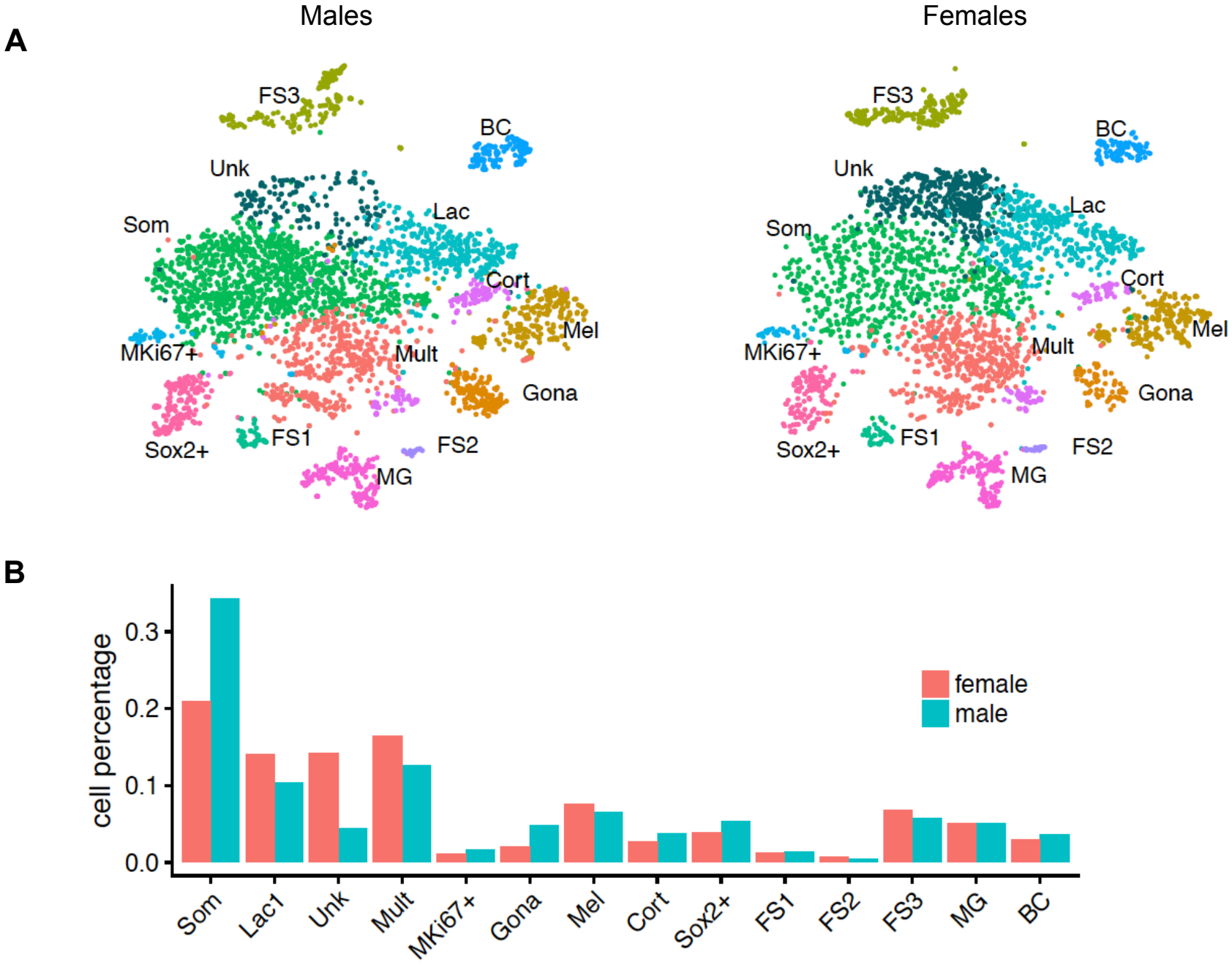
A
Males
Females
FS3
BC
Unk
Lac
Som
Cort
Mel
MKi67+
Mult
Gona
Sox2+
FS1
FS2
MG
B
cell percentage
0.0
0.1
0.2
0.3
female
male
Som
Lac1
Unk
Mult
MKi67+
Gona
Mel
Cort
Sox2+
FS1
FS2
FS3
MG
BC

Fig. 6

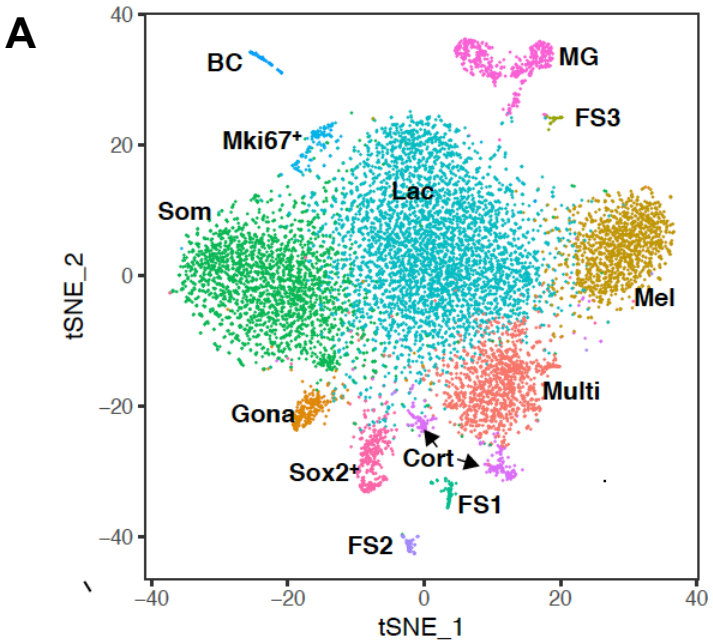
A
BC
MG
FS3
Mki67+
Lac
Som
Mel
Multi
Gona
Cort
Sox2+
FS1
FS2
tSNE_2
tSNE_1
40
20
0
−20
−40
−40
−20
0
20
40

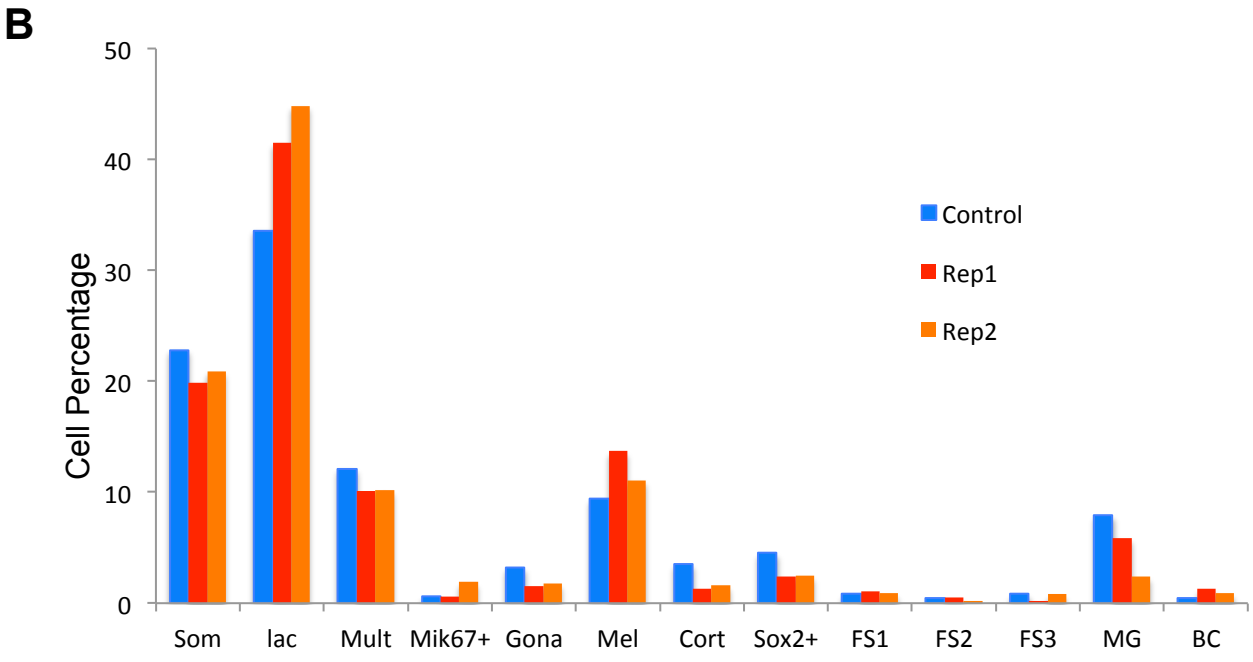
B
Cell Percentage
50
40
30
20
10
0
Control
Rep1
Rep2
Som
lac
Mult
Mik67+
Gona
Mel
Cort
Sox2+
FS1
FS2
FS3
MG
BC

Fig. 6

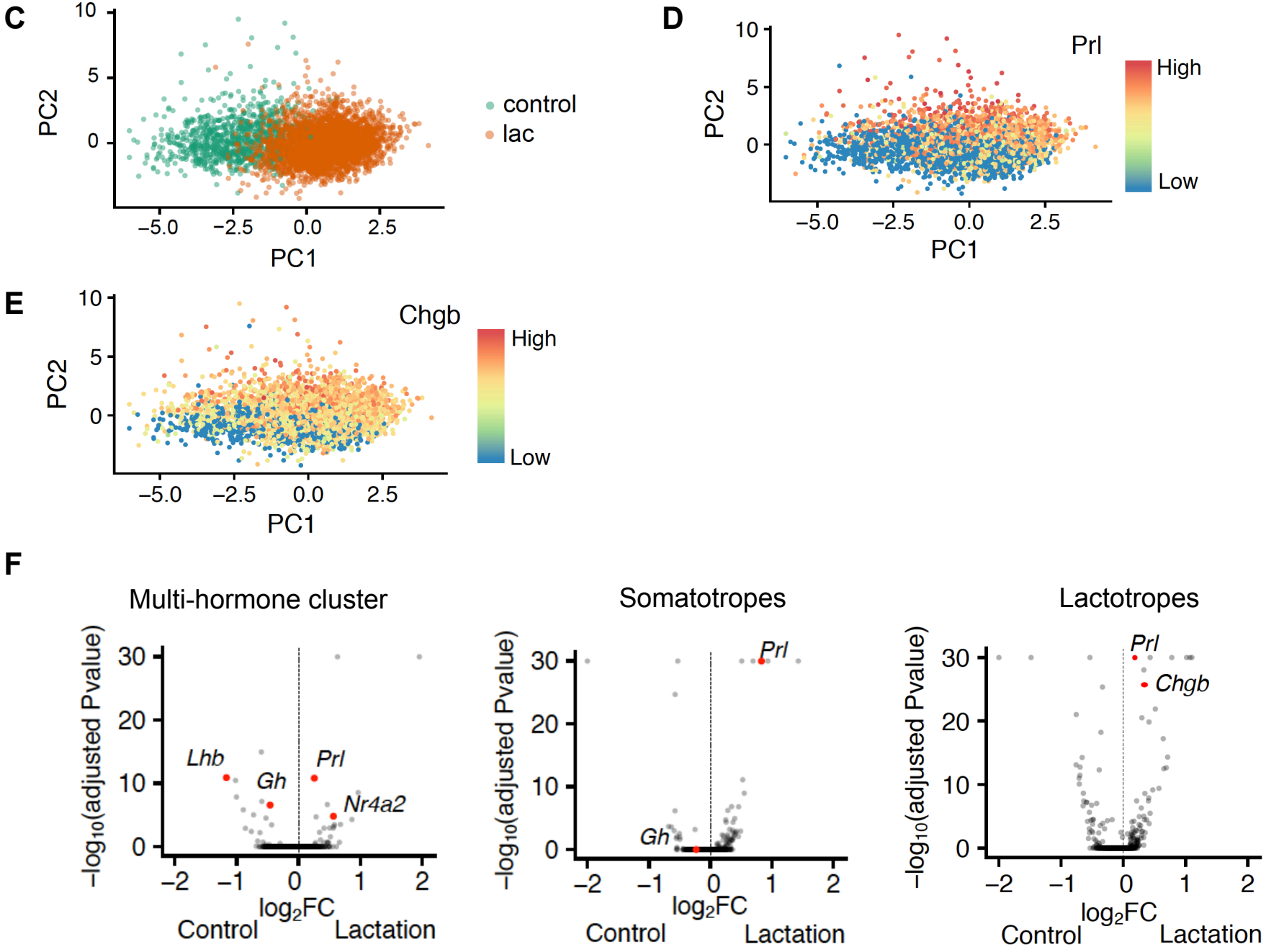
C
PC2
PC1
control
lac
D
Prl
High
Low
E
Chgb
F
Multi-hormone cluster
Somatotropes
Lactotropes
−log10(adjusted Pvalue)
log2FC
Control
Lactation
Lhb
Gh
Prl
Nr4a2
Chgb

Fig. 7

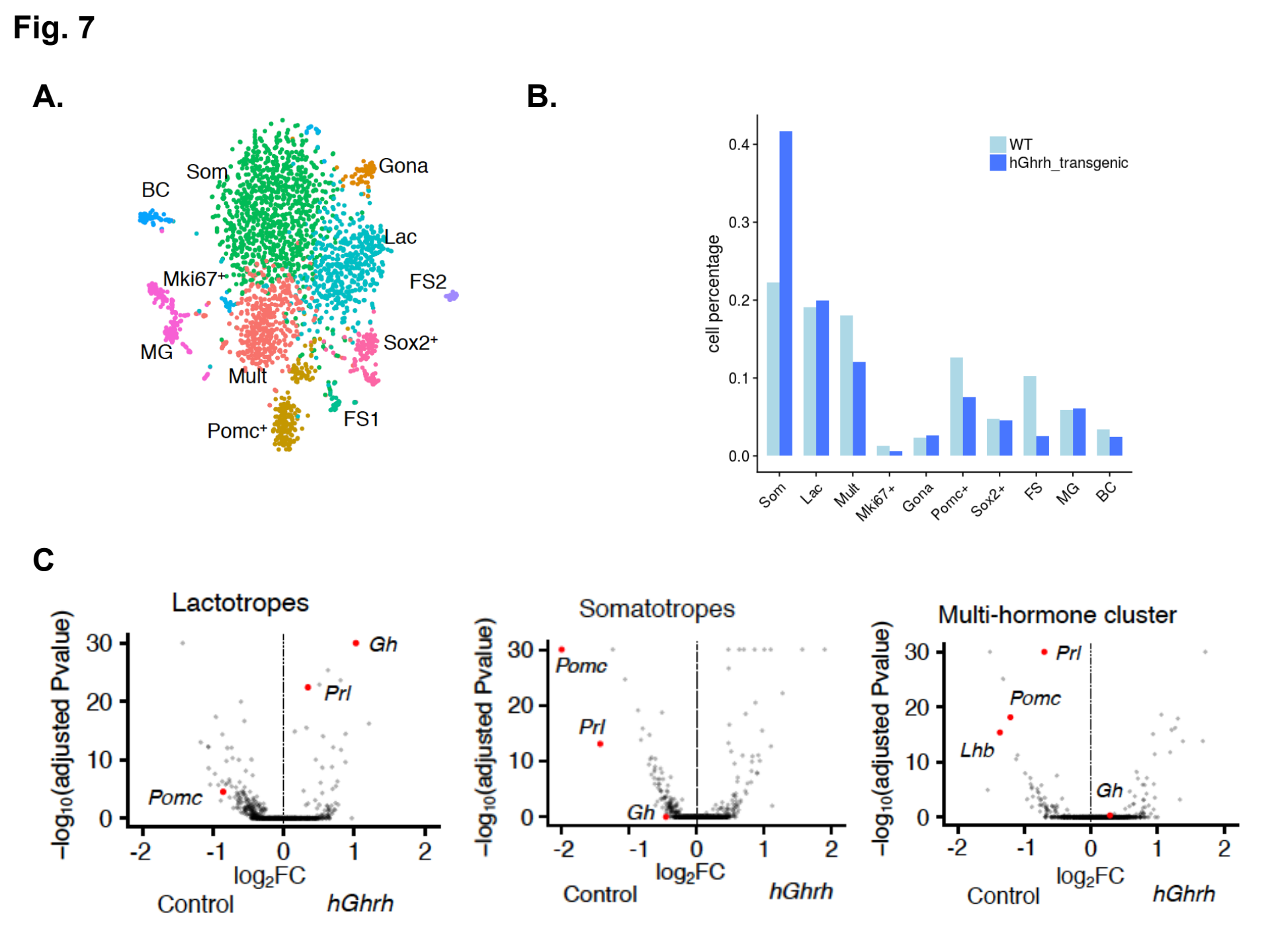
A.
Som
Gona
BC
Lac
Mki67+
FS2
Sox2+
MG
Mult
FS1
Pomc+
B.
WT
hGhrh_transgenic
cell percentage
0.4
0.3
0.2
0.1
0.0
Som
Lac
Mult
Mki67+
Gona
Pomc+
Sox2+
FS
MG
BC
C
Lactotropes
Somatotropes
Multi-hormone cluster
−log10(adjusted Pvalue)
log2FC
Control
hGhrh
Gh
Prl
Pomc
Lhb

Fig. S1

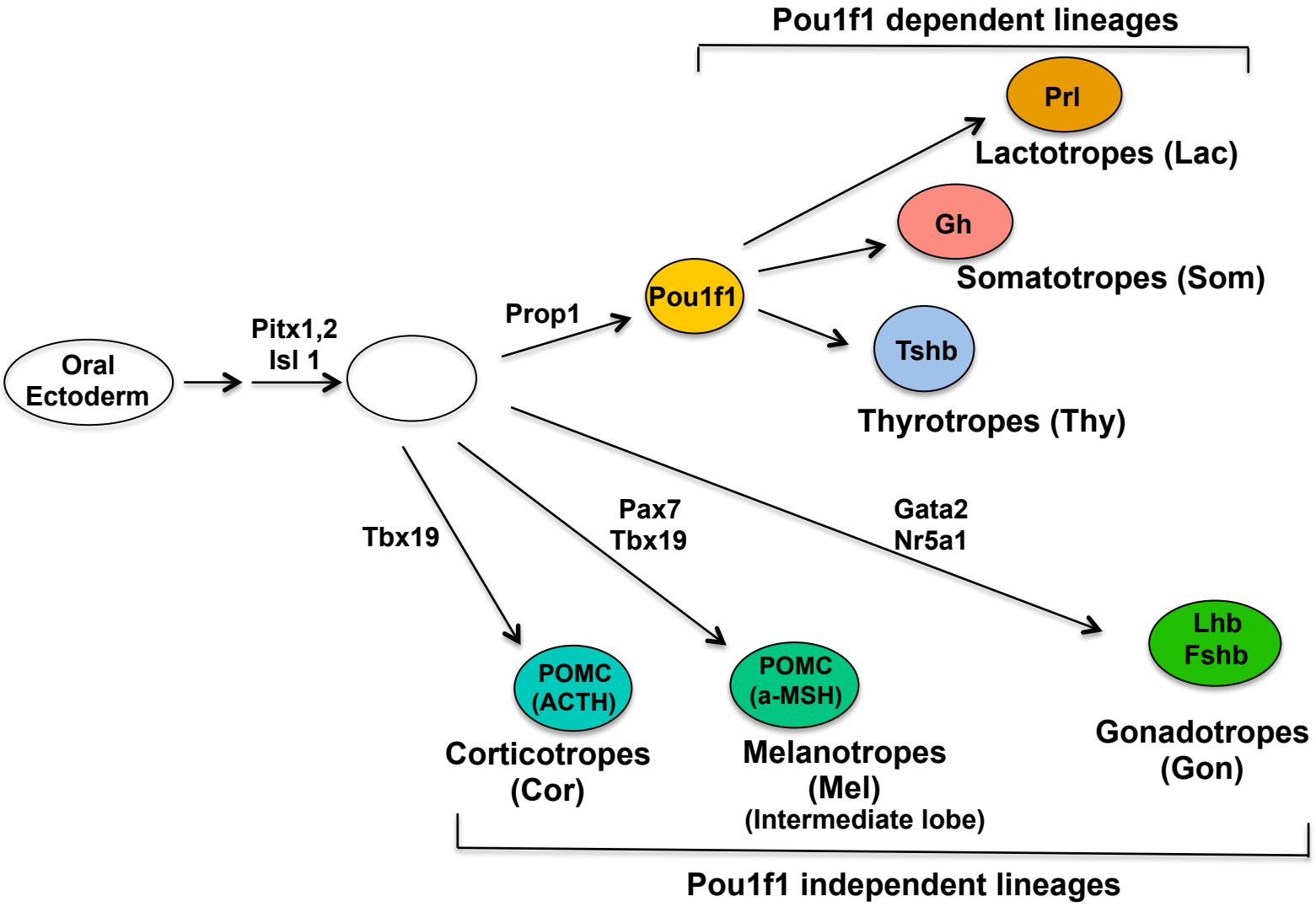
Pou1f1 dependent lineages
Prl
Lactotropes (Lac)
Gh
Somatotropes (Som)
Pou1f1
Prop1
Pitx1,2
Isl 1
Oral
Ectoderm
Tshb
Thyrotropes (Thy)
Tbx19
Pax7
Tbx19
Gata2
Nr5a1
POMC
(ACTH)
POMC
(a-MSH)
Lhb
Fshb
Corticotropes
(Cor)
Melanotropes
(Mel)
(Intermediate lobe)
Gonadotropes
(Gon)
Pou1f1 independent lineages

Fig. S2

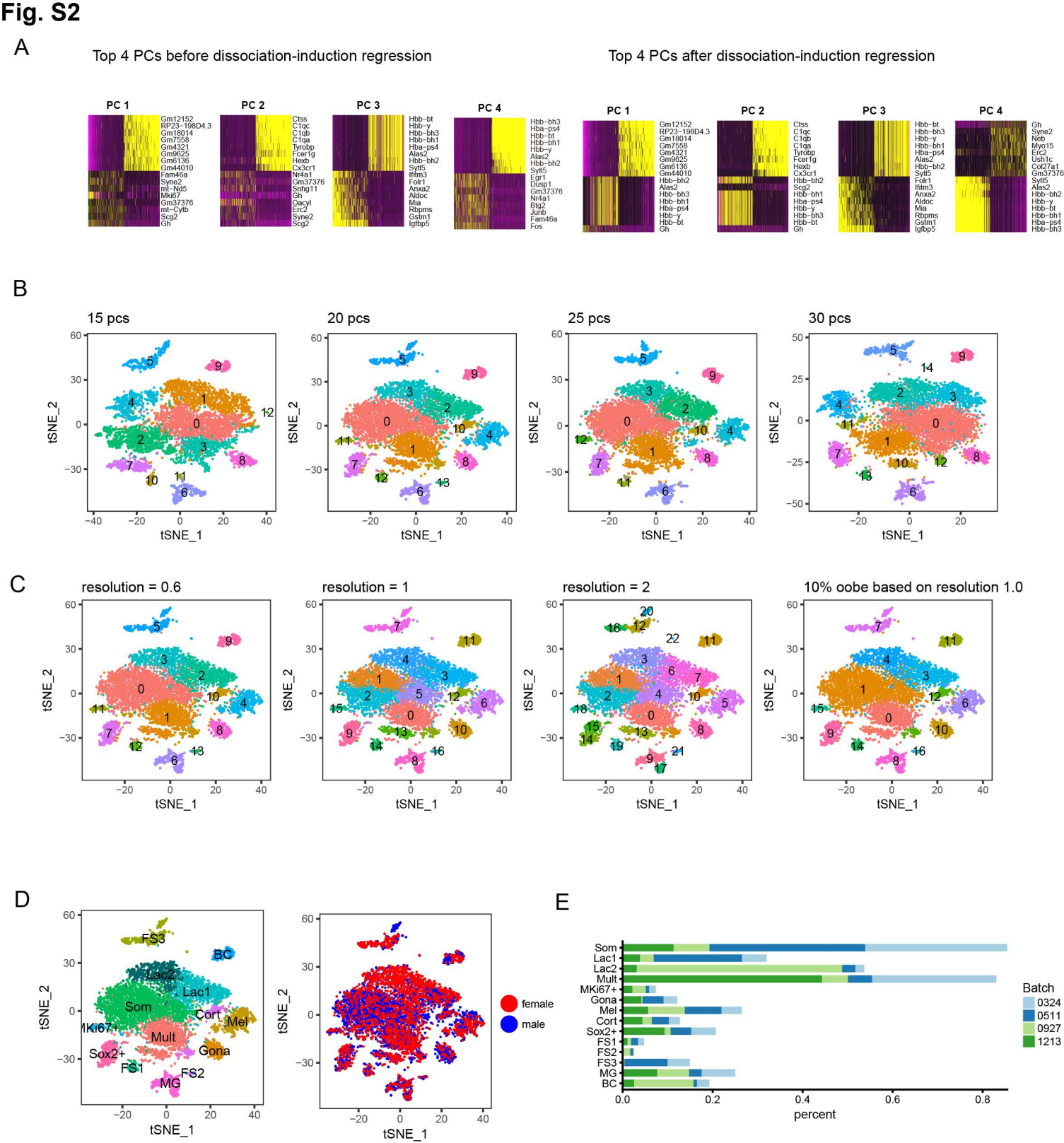
A
Top 4 PCs before dissociation-induction regression
Top 4 PCs after dissociation-induction regression
PC 1
PC 2
PC 3
PC 4
B
15 pcs
20 pcs
25 pcs
30 pcs
C
resolution = 0.6
resolution = 1
resolution = 2
10% oobe based on resolution 1.0
tSNE_1
tSNE_2
D
FS3
BC
Lac2
Lac1
Som
Cort
Mel
Mult
Gona
Sox2+
FS1
FS2
MG
female
male
E
Som
Lac1
Lac2
Mult
MKi67+
Gona
Mel
Cort
Sox2+
FS1
FS2
FS3
MG
BC
percent
Batch
0324
0511
0927
1213

Fig. S3

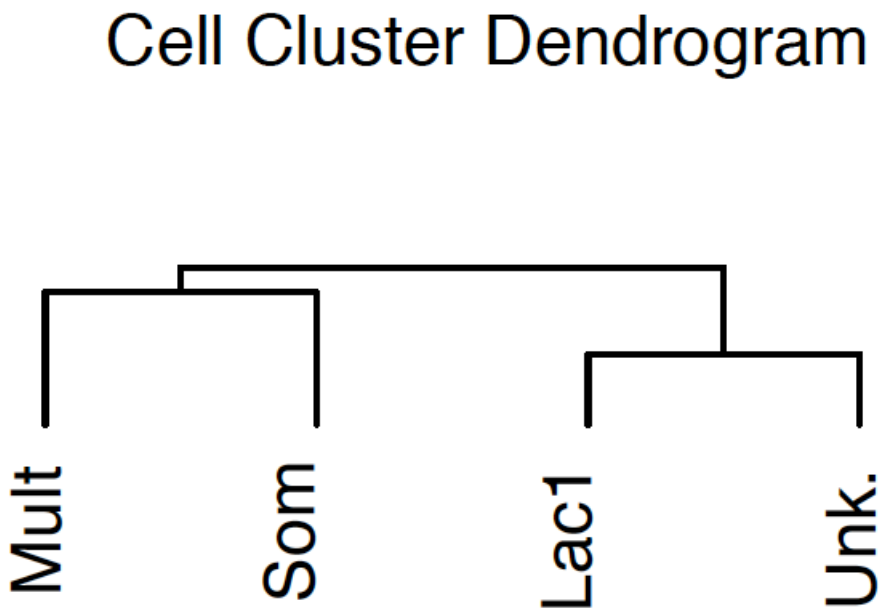

Fig. S4

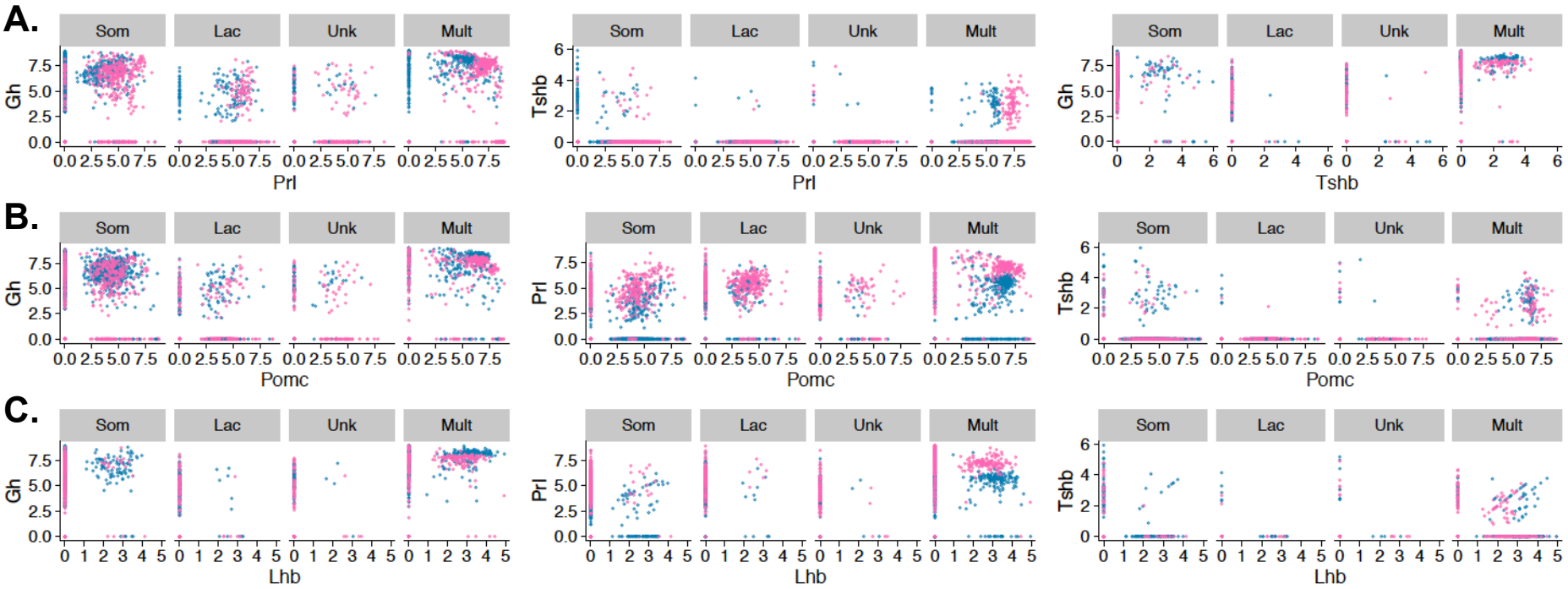

Fig. S5

A.

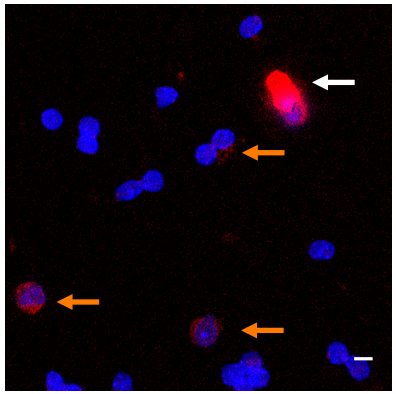

Gh RNA (Red)
DAPI (Blue)

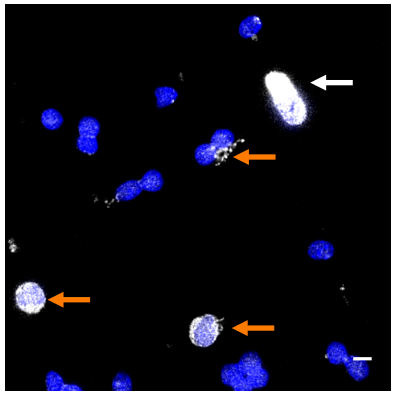

POMC RNA (Gray)
DAPI (Blue)

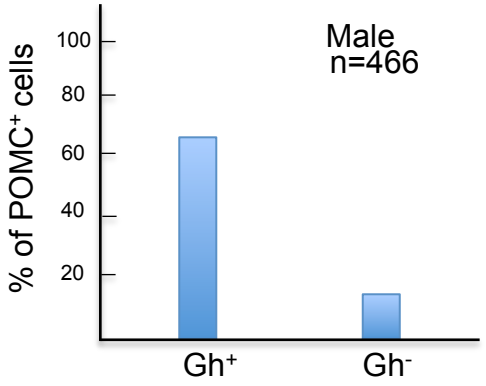

B.

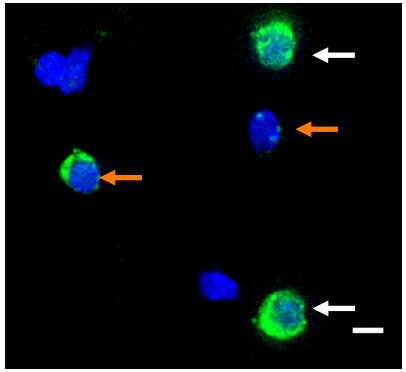

Prl RNA (Green)
DAPI (Blue)

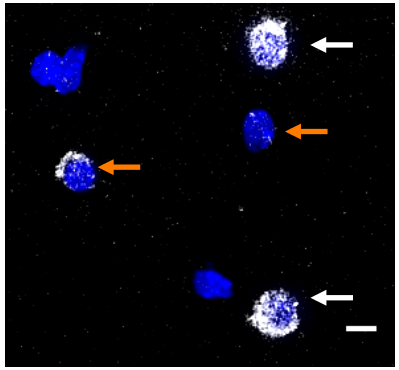

POMC RNA (Gray)
DAPI (Blue)

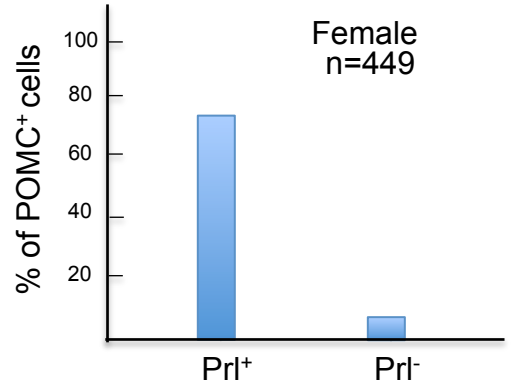

Fig. S6

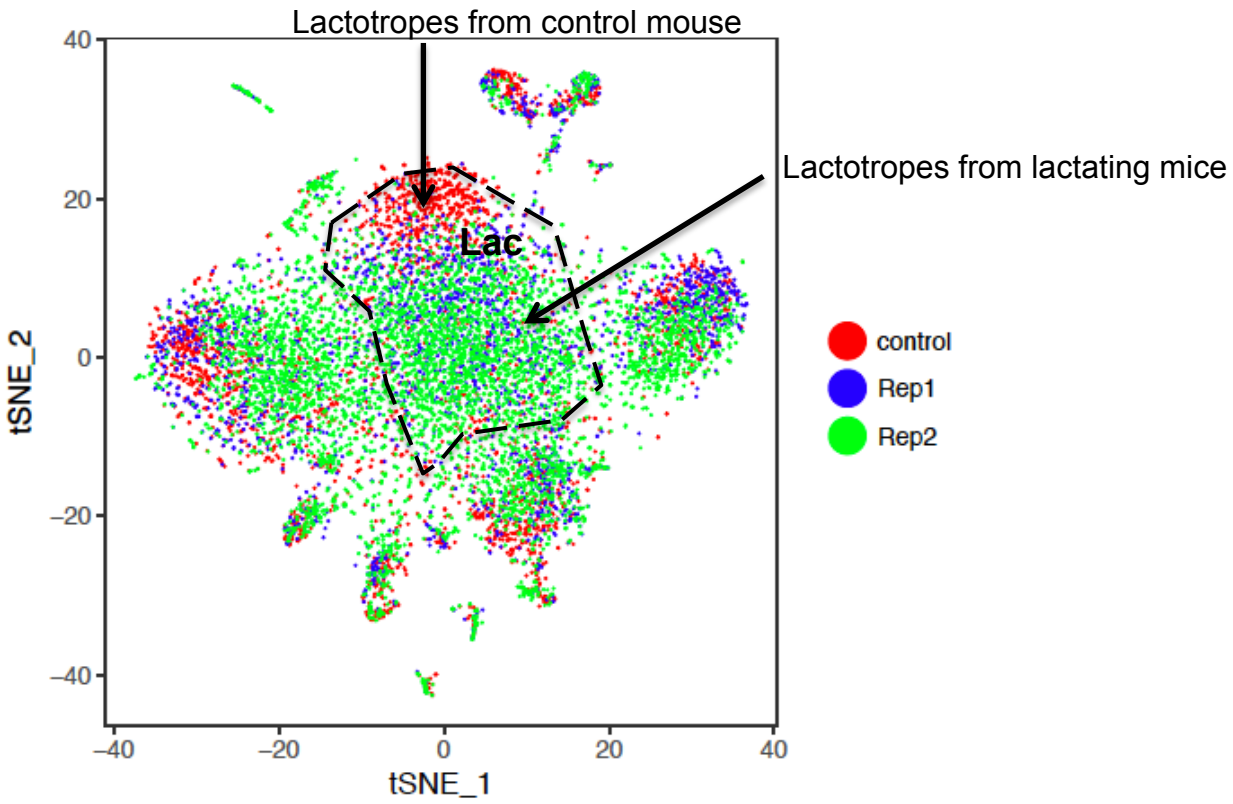
Lactotropes from control mouse
Lactotropes from lactating mice
Lac
tSNE_2
tSNE_1
40
20
0
−20
−40
−40
−20
0
20
40
control
Rep1
Rep2